

REFERENCES

- Ahmad, M.I., Zaidi, S.M.J., and Rahman, S.U. (2006). Proton conductivity and characterization of novel composite membranes for medium-temperature fuel cells. Desalination, 193, 387-397.
- Akbarian-Feizi, L., Mehdipour-Ataei, S., Yeganeh, H., (2010). Survey of sulfonated polyimide membrane as a good candidate for nafion substitution in fuel cell. International journal of Hydrogen Energy, 35, 9385-9397.
- Andújar, J.M., and Segura, F. (2009). Fuel cells: History and updating. A walk along two centuries. Renewable and Sustainable Energy Reviews, 13, 2309-2322.
- Bhuvana, S., Madhumathi, M., and Sarojadevi, M. (2006). Synthesis and characterization of processable heat resistant poly (amide-imide) for high temperature applications. Polymer Bulletin, 57, 61-72.
- Bhuvana, S., and Sarojadevi, M. (2007). Synthesis and characterization of poly (amide-imide-imide)s based on diacids with bulky m-chloro phenyl moiety and rigid pyridine moiety. Journal of Polymer Research, 14, 261-267.
- Cheng, L., and Jian, X. (2004). Synthesis of new aromatic poly(amide imide)s from unsymmetrical extended diamine containing a phthalazinone moiety. Chinese Journal of Polymer Science, 22(4), 389-393.
- EG&G Services, Parsons, Inc., Science Applications International Corporation. (2000). Fuel Cell Handbook (Fifth Edition). Springfield, VA: National Technical Information Service, U.S. Department of Commerce.
- Einsla, B.R., Kim, Y.S., Hickner, M.A., Hong, Y.-T., Hill, M.L., Pivovar, B.S., and McGrath, J.E. (2005). Sulfonated naphthalene dianhydride based polyimide copolymers for proton-exchange-membrane fuel cells II. Membrane properties and fuel cell performance. Journal of Membrane Science, 255, 141-148.
- Fang, X., Wang, Z., Yang, Z., Gao, L., Li, Q., and Ding, M. (2003). Novel polyimides derived from 2,3,3',4'-benzophenonetetracarboxylic dianhydride. Polymer, 44, 2641-2646.

- Feng, S., Shang, Y., Wang, Y., Liu, G., Xie, X., Dong, W., Xu, J., and Mathur, V.K. (2010). Synthesis and crosslinking of hydroxyl-functionalized sulfonated poly(ether ether ketone) copolymer as candidates for proton exchange membranes. *Journal of Membrane Science*, 352, 14-21.
- García, J.M., García, F.C., Serna, F., and Peña, J.L. (2009). High-performance aromatic poly amides. *Progress in Polymer Science*, Article in press.
- Guo, Q., Pintauro, P.N., Tang, H., and O'Connor, S. (1999). Sulfonated and crosslinked polyphosphazene-based proton-exchange membranes. *Journal of Membrane Science*, 154, 175-181.
- Hsiao, S.-H., Yang, C.-P., Chen, C.-W., and Liou, G.-S. (2005). Synthesis and properties of novel poly(amide-imide)s containing pendent diphenylamino groups. *European Polymer Journal*, 41, 511-517.
- Javaid Zaidi, S.M. (2003). Polymer sulfonation - a versatile route to prepare proton-conducting membrane material for advanced technologies. *The Arabian Journal for Science and Engineering*, 28(2B), 183-194.
- Jonquières, A., Clément, R., and Lochon, P. (2005). New film-forming poly(urethane-amide-imide) block copolymer: influence of soft block on membrane properties for the purification of a fuel octane enhancer by pervaporation. *European Polymer Journal*, 41, 783-795.
- Kamarudin, S.K., Achmad, F., and Daud, W.R.W. (2009). Overview on the application of direct methanol fuel cell (DMFC) for portable electronic devices. *International Journal of Hydrogen Energy*, 34, 6902-6916.
- Kausar, A., Zulfiqar, S., Ahmad, Z., and Sarwar, M.I. (2010). Novel processable and heat resistant poly(phenylthiourea azomethine imide)s: synthesis and characterization. *Polymer Degradation and Stability*, 95, 1826-1833.
- Kirubakaran, A., Jain, S., and Nema, R.K. (2009). A review on fuel cell technologies and power electronic interface. *Renewable and Sustainable Energy Reviews*, 13, 2430-2440.
- Li, W., Cui, Z., Zhou, X., Zhang, S., Dai, L., and Xing, W. (2008). Sulfonated poly(arylene-co-imide)s as water stable proton exchange membrane materials for fuel cells. *Journal of Membrane Science*, 315, 172-179.

- Li, T., Zhong, G., Fu, R., and Yang, Y. (2010). Synthesis and characterization of Nafion/cross-linked PVP semi-interpenetrating polymer network membrane for direct methanol fuel cell. *Journal of Membrane Science*, 354, 189-197.
- Meyer, G., Gebel, G., Gonao, L., Capron, P., Marscaq, D., Marestin, C., and Mercier, R. (2006). Degradation of sulfonated polyimide membranes in fuel cell conditions. *Journal of Power Sources*, 157, 293-301.
- Ng, F., Jones, D.J., Rozière, J., Bauer, B., Schuster, M., and Jeske, M. (2010). Novel sulfonated poly(arylene ether benzimidazole) Cardo proton conducting membranes for PEMFC. *Journal of Membrane Science*, 362, 184-191.
- Nguyen, T., Wang, X. (2010). Multifunctional composite membrane based on a highly porous polyimide matrix for direct methanol fuel cells. *Journal of Power Sources*, 195, 1024-1030.
- Pan, H., Zhu, X., and Jian, X. (2010). Synthesis and properties of sulfonated copoly(phthalazinone ether imides) as electrolyte membranes in fuel cells. *Electrochimica Acta*, 55, 709-714.
- Peighambarioust, S.J., Rowshanzamir, S., and Amjadi, M. (2010). Review of the proton exchange membranes for fuel cell applications. *International Journal of Hydrogen Energy*, 35, 9349-9384.
- Pinto, B.P., M, L.C.S., Sena, M.E. (2007). Sulfonated poly(ether imide): A versatile route to prepare functionalized polymers by homogenous sulfonation. *Material Letters*, 61, 2540-2543.
- Rahimpour, A., Madaeni, S.S., and Mehdipour-Ataei, S. (2008). Synthesis of a novel poly(amide-imide) (PAI) and preparation and characterization of PAI blended polyethersulfone (PES) membrane. *Journal of Membrane Science*, 311, 349-359.
- Reyna-Valencia, A., Kaliaguine, S., and Bousmina, M. (2006). Structural and mechanical characterization of poly(ether ether ketone) (PEEK) and sulfonated PEEK films: effects of thermal history, sulfonation, and preparation conditions. *Journal of Applied Polymer Science*, 99, 756-774.
- Sammes, N.M. (2006). *Fuel Cell Technology: Reaching towards Commercialization*. Germany: Springer Science+Business Media.

- Sang, Y., Xie, X., Jin, H., Guo, J., Wang, Y., Feng, S., Wang, S., and Xu, J. (2006). Synthesis and characterization of novel sulfonated naphthalenic polyimides as proton conductive membrane. *European Polymer Journal*, 42, 2987-2993.
- Shabani, I., Hasani-Sadrabadi, M.M., Haddadi-Asl, V., and Soleimani, M. (2011). Nanofiber-based polyelectrolytes as novel membranes for fuel cell applications. *Journal of Membrane Science*, 368, 233-240.
- Somboonsub, B., Srisuwan, S., Invernale, M.A., Thongyai, S., Praserthdam, P., Scola, D. A., Sotzing, C.A. (2010). Comparison of the thermally stable conducting polymers PEDOT, PANi, and PPy using sulfonated poly(imide) templates. *Polymer*, 51, 4472-4476.
- Sung, K.A., Cho, K.Y., Kim, W.K., and Park, J.K. (2010). Sulfonated polyimide membrane coated with crosslinkable layer for direct methanol fuel cell. *Electrochimica Acta*, 55, 995-1000.
- Vora, R.H., and Goh, S.H. (2006). Designed poly(ether-imide)s and fluorocopoly(ether-imide)s: Synthesis, characterization and their film properties. *Materials Science and Engineering B*, 132, 24-33.
- Wang, Y., Goh, S.H., and Chung, T.-S. (2007). Miscibility study of Torlon® polyamide-imide with Matrimid® 5218 polyimide and polybenzimidazole. *Polymer*, 48, 2901-2909.
- Woo, Y., Oh, S.Y., Kang, Y.S., and Jung, B. (2003). Synthesis and characterization of sulfonated polyimide membranes for direct methanol fuel cell. *Journal of Membrane Science*, 220, 31-45.
- Xue, S., Yin, G., Cai, K., and Shao, Y. (2007). Permeabilities of methanol, ethanol and dimethyl ether in new composite membranes: a comparison with Nafion membranes. *Journal of Membrane Science*, 289, 51-57.
- Yang, C.-C., Lee, Y.-J., and Yang, J.M. (2009). Direct methanol fuel cell (DMFC) based on PVA/MMT composite polymer membranes. *Journal of Power Sources*, 188, 30-37.
- Zhu, X., Pan, H., Liang, Y., and Jian, X. (2008). Synthesis and properties of novel sulfonated polyimides containing phthalazinone moieties for PEMFC. *European Polymer Journal*, 44, 3782-3789.

APPENDICES

Appendix A FT-IR Spectrum

FT-IR spectrometer (Thermo Nicolet, Nexus 670) was used to measure spectra of 4,4'-diaminodiphenylmethane (DDM), 4,4'-diaminodiphenylmethane-2,2'-disulfonic acid disodium salt (S-DDM), 3,3',4,4'-benzophenonetetracarboxylic dianhydride (BPTDA), adipic acid dihydrazide (ADH) and sulfonated poly(aromatic imide-*co*-aliphatic imide) (S-coPI). The spectrometer was operated in the absorption mode with 64 scans and a resolution of 4 cm^{-1} , covering a wavenumber range of $4000 - 400\text{ cm}^{-1}$. Optical grade KBr was used as the background material. DDM, S-DDM, BTDA and ADH were mixed with dried KBr before the measurements. ZnSe was used as a background material for S-coPI. ZnSe was coated with S-coPI solution and dried before the measurements.

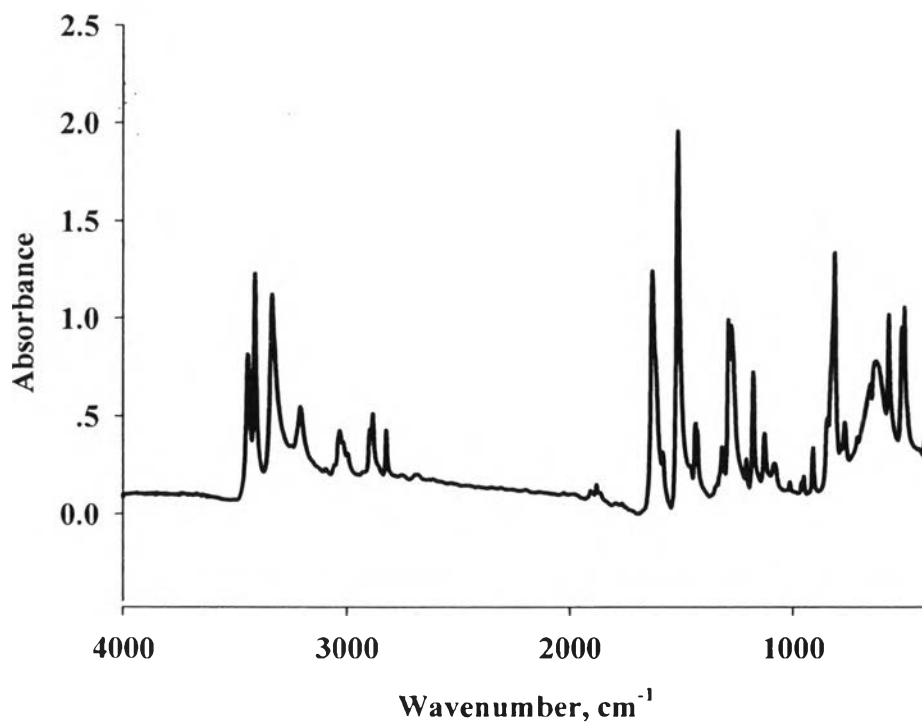


Figure A1 FT-IR spectrum of 4,4'-diaminodiphenylmethane (DDM).

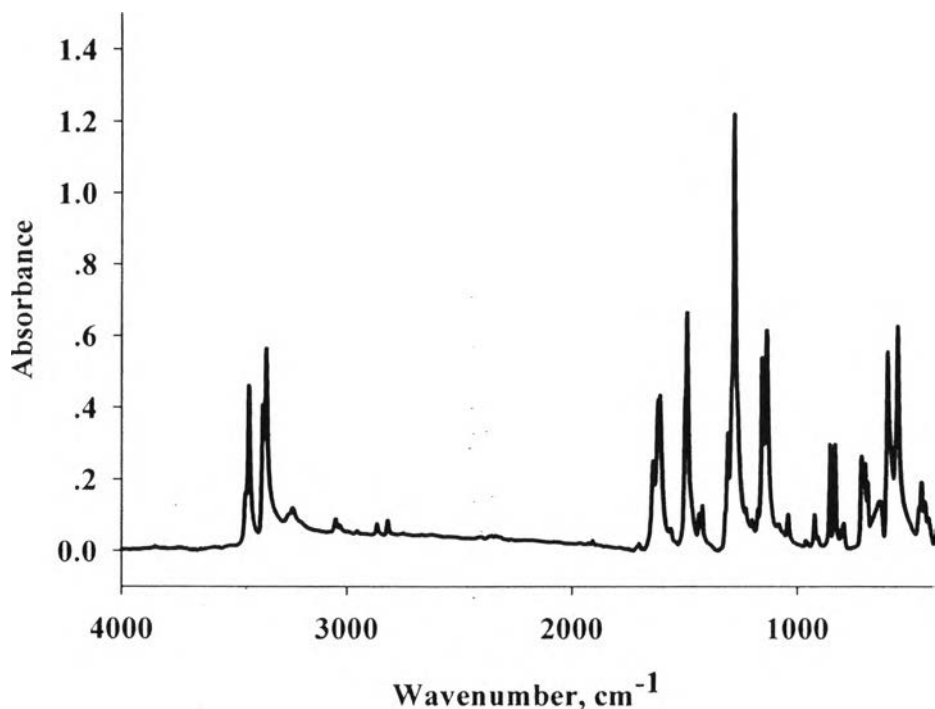


Figure A2 FT-IR spectrum of 4,4'-diaminodiphenylmethane-2,2'-disulfonic acid disodium salt (S-DDM).

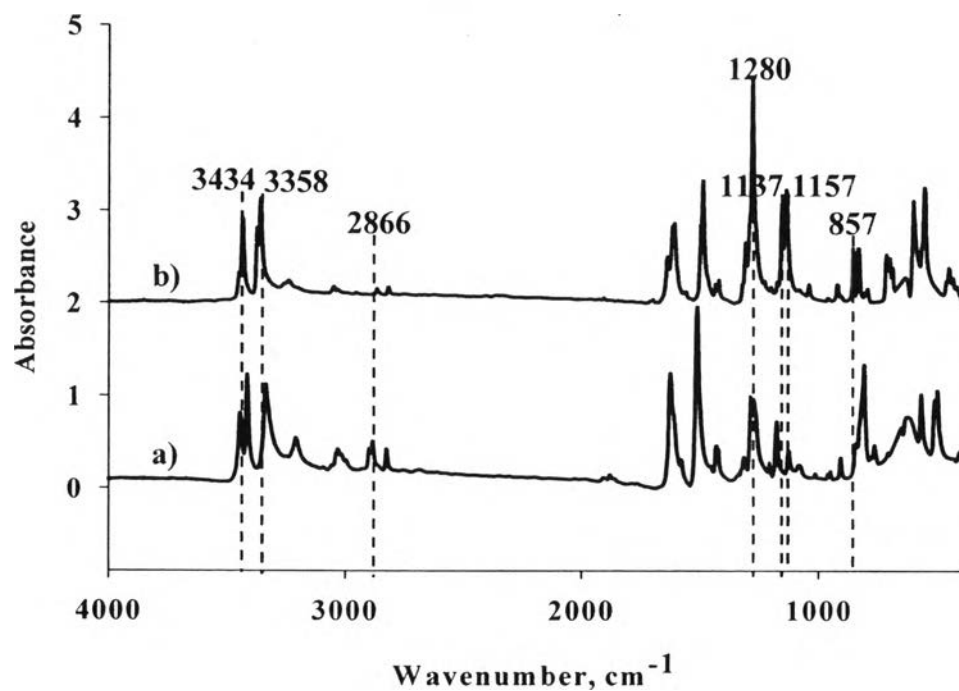


Figure A3 FT-IR spectra of: a) DDM; and b) S-DDM.

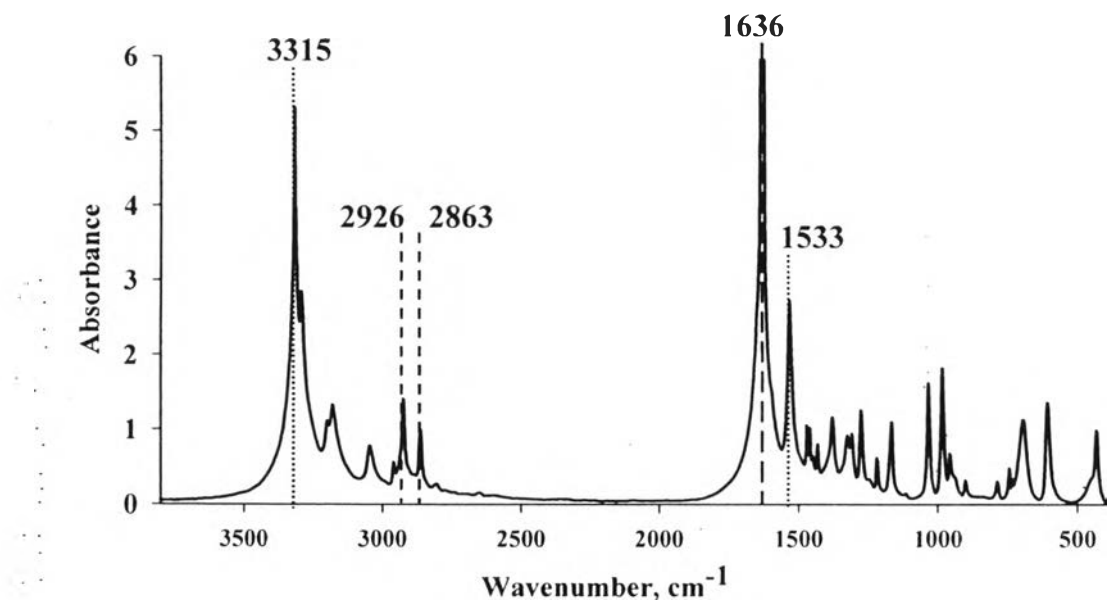


Figure A4 A FT-IR spectrum of adipic acid dihydrazide (ADH).

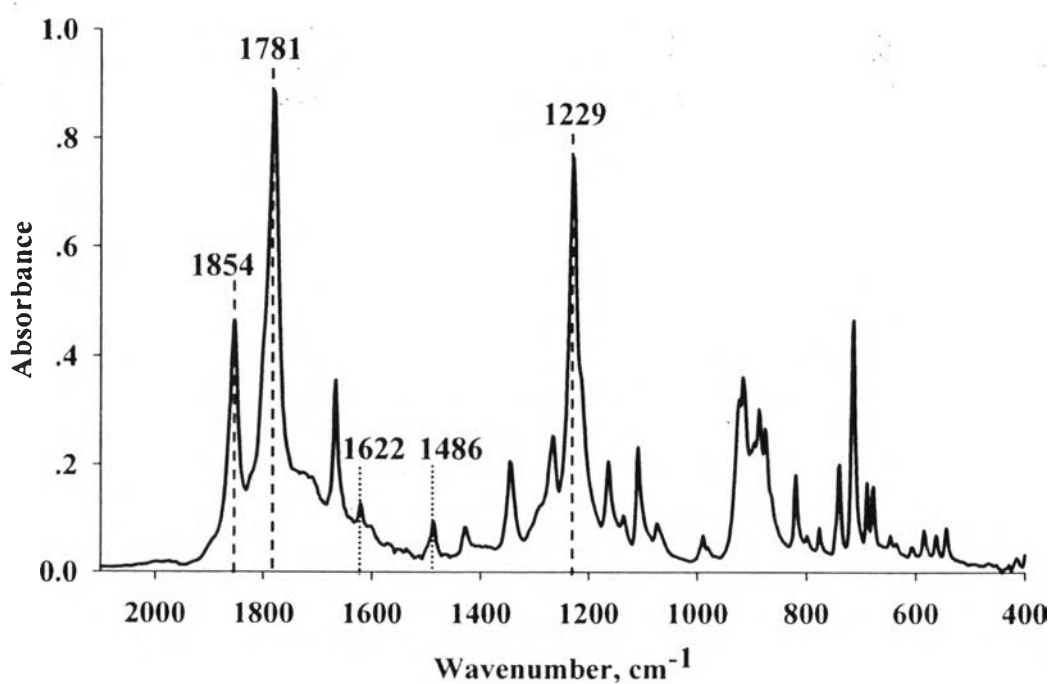


Figure A5 A FT-IR spectrum of 3,3',4,4'-benzophenonetetracarboxylic dianhydride (BPTDA).

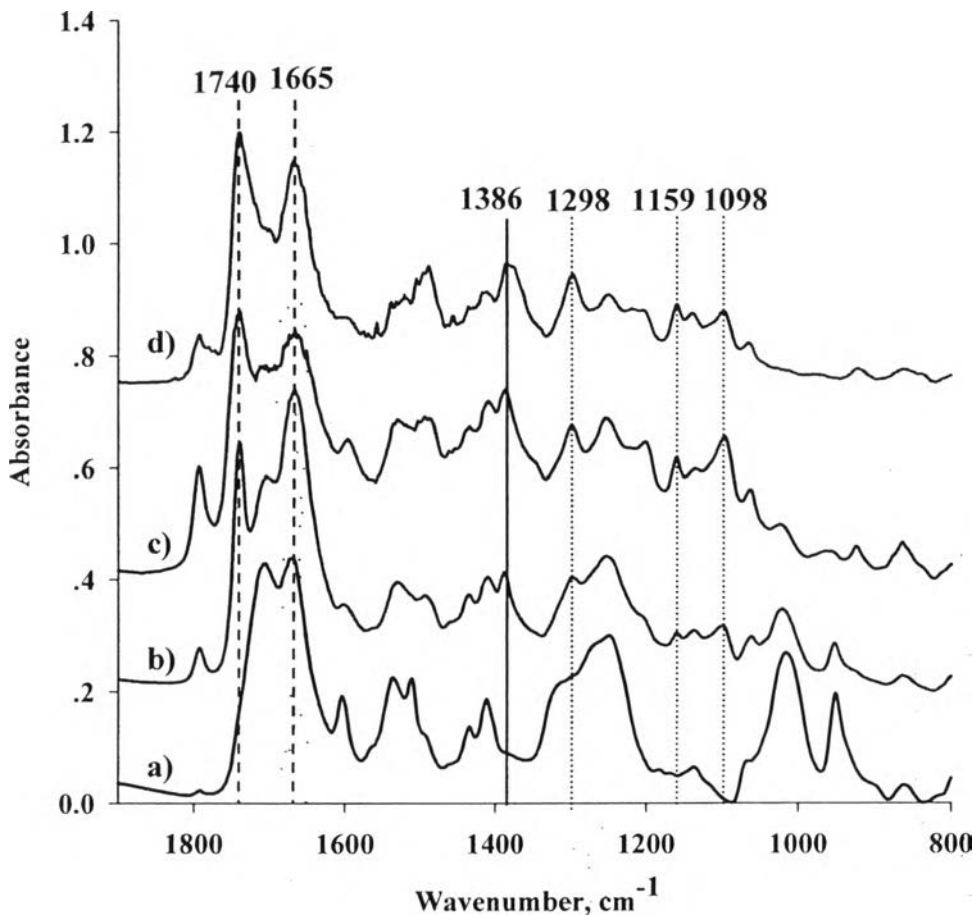


Figure A6 FT-IR spectra of: a) Non S-coPI; b) S-coPI-1; c) S-coPI-2; d) S-coPI-3.

The absorption infrared spectra of DDM and S-DDM are shown in Figure A3. The absorption bands at 3434 cm^{-1} and 3358 cm^{-1} can be assigned to the primary amine group. The peak at 2866 cm^{-1} is assigned to the C-H stretching of the methylene group, 1280 cm^{-1} and 1157 cm^{-1} are assigned to the S=O of the sulfonic group not present in DDM, 1137 cm^{-1} and 857 cm^{-1} are assigned to the S-O stretching of the sulfonated group not present in DDM. (Vora *et al.*, 2006 and Zhu *et al.*, 2008)

Figure A4 shows the IR spectrum of ADH. Absorption band at 3315 cm^{-1} is assigned to the N-H stretching of amide, 2926 cm^{-1} and 2863 cm^{-1} are assigned to the C-H stretching of alkanes, 1636 cm^{-1} is assigned to the carbonyl group (C=O) of amide, and 1533 cm^{-1} is assigned to the N-H bending of amide.

Figure A5 shows the IR spectrum of BTDA. Absorption band at 1854 cm^{-1} is assigned to the asymmetric stretching of the carbonyl group ($\text{C}=\text{O}$) of anhydride, 1781 cm^{-1} is assigned to the symmetric stretching of the carbonyl group ($\text{C}=\text{O}$) of anhydride, 1622 cm^{-1} and 1486 cm^{-1} are assigned to the $\text{C}=\text{C}$ stretching of aromatic, and 1229 cm^{-1} is assigned to the $\text{C}-\text{O}$ stretching of anhydride.

Figure A6 shows the IR spectrum of S-coPI of various sulfonation degrees. Absorption band at 1740 cm^{-1} is assigned to the asymmetric stretching of carbonyl group ($\text{C}=\text{O}$) of the imido ring, 1665 cm^{-1} is assigned to the symmetric stretching of the carbonyl group ($\text{C}=\text{O}$) of the imido ring, 1386 cm^{-1} is assigned to the $\text{C}-\text{N}-\text{C}$ stretching of the imide ring (for non sulfonated coPI is shown at 1412 cm^{-1}). The peaks at 1298 cm^{-1} , 1159 cm^{-1} and 1098 cm^{-1} are assigned to the sulfonic group ($\text{S}=\text{O}$ and $\text{S}-\text{O}$) (Vora *et al.*, 2006 and Zhu *et al.*, 2008).

Appendix B Thermogravimetric Analysis (TGA)

The thermogravimetric analysis (Perkins Elmer, Pyris Diamond TG/DTA) was carried out to determine the thermal stability of the polymer membrane. The experiment was carried out by weighting a film sample of 2 - 4 mg and placed it in an alumina pan, and then it was heated under a nitrogen atmosphere with the heating rate of 10 °C/min in the temperature range of 50 - 800 °C. All the samples were dried at 100 °C for 24 h before the measurements.

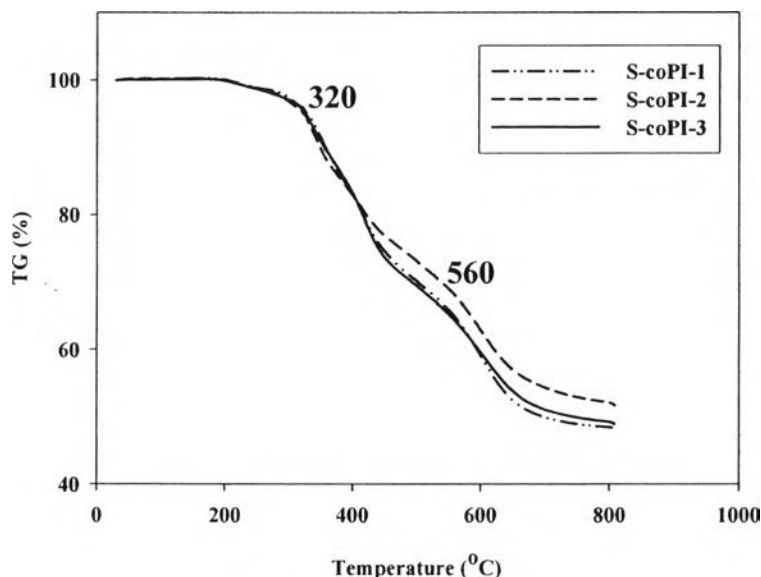


Figure B1 The thermogravimetric analysis curves of S-coPI membranes.

The thermal property of S-coPI is shown in Figure B1; the weight loss at about 320 °C is assigned to the decomposition of the sulfonated group. The weight loss due to degradation of backbone structure appears at 560 °C. The decomposition of each polymer molecule due to the bond dissociation energy, the bond energy of C–S and C–C are about 272 and 348 kJ/mol, respectively. So the sulfonated group connected with the C–S bond is decomposed before the C–C backbone. However, the polymer structure contains the N–N bond whose bond energy is only 170 kJ/mol; this is the lowest bond energy of this polymer structure, and this bond is broken before the C–S bond. Therefore, the polymer structure should not contain the N–N bond for further development in the future.

Appendix C Methanol Permeability

The methanol permeability of the membranes was determined by using the two compartments diffusion cell technique. One compartment ($V_A = 250$ ml) was filled with a solution of 2.5 M methanol. The other compartment ($V_B = 250$ ml) was filled with deionized water. The membrane was clamped between the two compartments. Methanol will flow across the membrane due to the methanol concentration difference between the compartment A and the compartment B. The methanol permeation in the compartment B as a function of time is given by equation (C1):

$$P \text{ (cm}^2/\text{s}) = \frac{k_B \times V_B \times L}{A \times (C_A - C_B)} \quad (\text{C1})$$

where P = the methanol permeability

C_A = the methanol concentrations in the compartment A

C_B = the methanol concentrations in the compartment B

A = the area of a membrane

L = the thickness of a membrane

V_B = the volume of the solution in the compartment B

k_B = the slope of methanol concentration profile in the compartment B

The methanol concentrations were measured by using a PR2100 gas chromatography fitted with a Thermal Conductivity Detector (TCD); 2.5M ethanol was used as the internal standard.

Table C1 Methanol permeability of the S-coPI and Nafion117 membrane

Sample	Methanol permeability (10^{-8}) (cm^2/s)		
	No.1	No.2	Average
Non S-coPI	3.86	3.3	3.58 ± 0.39
S-coPI-1	5.60	6.11	5.85 ± 0.36
S-coPI-2	6.52	7.52	7.02 ± 0.71
S-coPI-3	4.32	3.72	4.02 ± 0.42
Nafion117	174	-	174

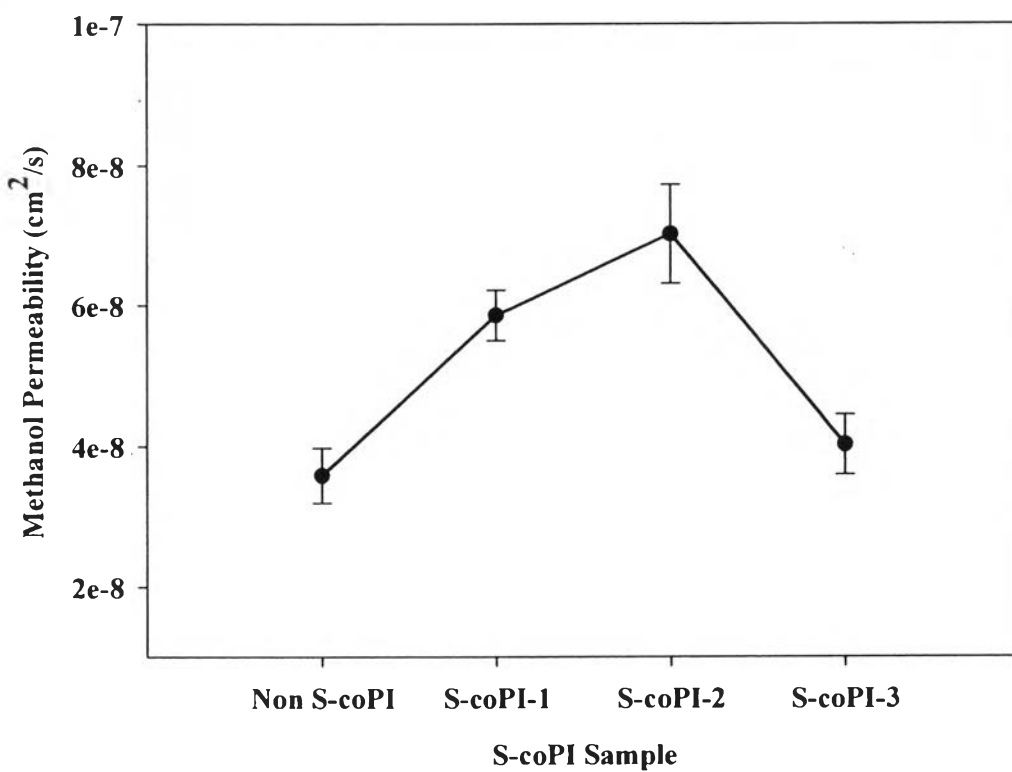
**Figure C1** Methanol permeability of Non S-coPI and S-coPI membranes.

Table C2 Raw data of internal standard curve of methanol concentration

MeOH Concentration	Peak area of MeOH		Peak area of EtOH		Peak area ratio	
	No.1	No.2	No.1	No.2	No.1	No.2
0 M	0	0	2451.57	2356.09	0	0
0.0001 M	0.48	0.37	3254.14	2328.81	0.000148	0.000159
0.001 M	1.29	1.45	2255.64	2713.02	0.000572	0.000534
0.01 M	4.8	6.99	2671.15	2318.44	0.001797	0.003015
0.05 M	39.54	53.18	2779.24	3494.72	0.014227	0.015217
0.1 M	66.7	63.26	2251.94	2054.48	0.029619	0.030791
0.5 M	324.82	389.44	2102.52	2402.63	0.154491	0.162089
1 M	756.71	640.04	2576.57	2102.08	0.293689	0.304479
2 M	1324.12	1439.36	2309.63	2347.55	0.573304	0.613133
2.5 M	1565.69	1727.52	2125.67	2248.69	0.736563	0.768234
3 M	1541.67	2207.33	1822.27	2322.29	0.846016	0.950497

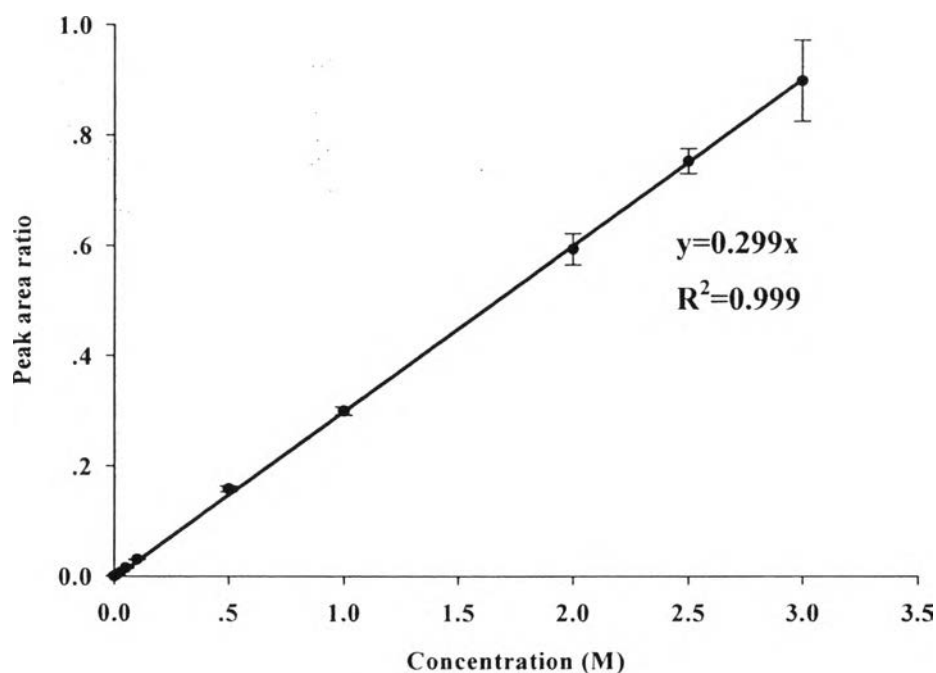
**Figure C2** Internal standard curve of methanol concentration.

Table C3 Raw data of methanol permeability calculation of Non S-coPI

No.1 Thickness 152.80 μm			No.2 Thickness 138.71 μm		
Time (second)	MeOH concentration (M)		Time (second)	MeOH concentration (M)	
	Comp. A	Comp. B		Comp. A	Comp. B
0	2.49280178	0	0	2.49201438	0
25200	2.46603995	0.00362712	14400	2.37979875	0.00240928
86400	2.40092762	0.010370234	25200	2.42780807	0.00370819
115200	2.46905434	0.013105389	82800	2.43319898	0.01016087
162000	2.46164641	0.020537178	100800	2.47356829	0.01255020
189000	2.45167293	0.024473786	165600	2.45203646	0.02158942
255600	2.48297440	0.03172729	181800	2.43998647	0.02201245

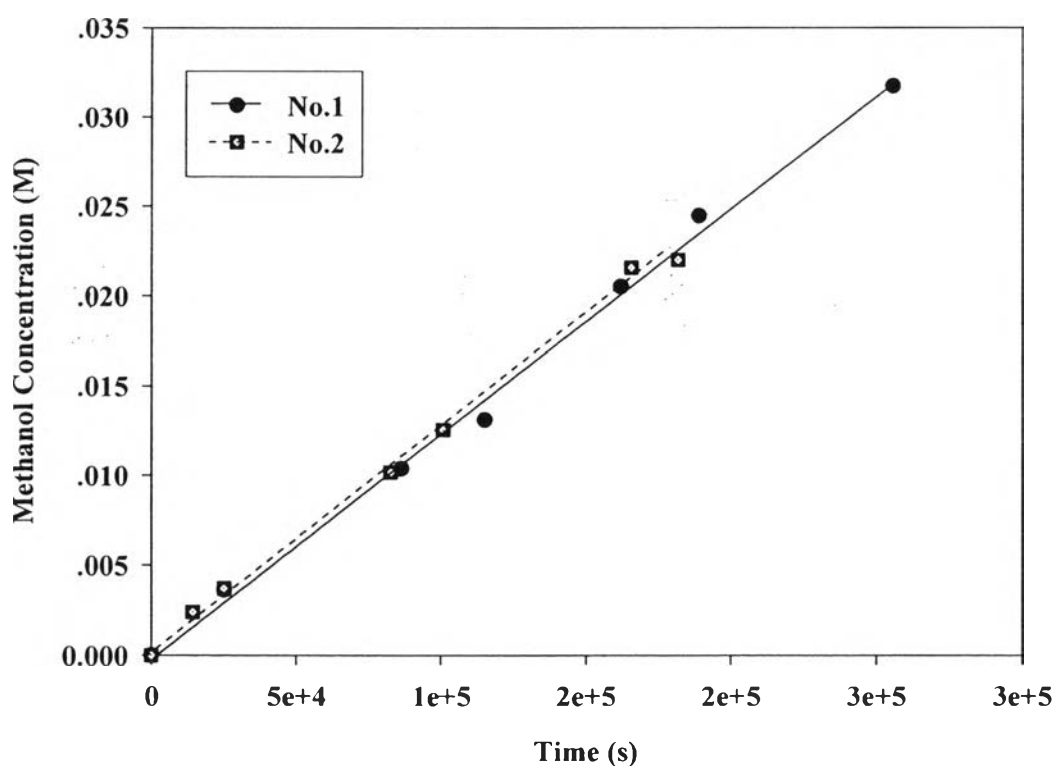
**Figure C3** Methanol concentration (M) in compartment B vs. time(s) of Non S-coPI.

Table C4 Raw data of methanol permeability calculation of S-coPI-1

No.1 Thickness 163.67 μm			No.2 Thickness 144.17 μm		
Time (second)	MeOH concentration (M)		Time (second)	MeOH concentration (M)	
	Comp. A	Comp. B		Comp. A	Comp. B
0	2.50455181	0	0	2.47115804	0
86400	2.44072832	0.01450771	25200	2.49969531	0.00565111
111600	2.38586010	0.01980414	86400	2.40558716	0.01665537
172800	2.46205575	0.02702685	100800	2.47600237	0.01927287
194400	2.47545845	0.03392855	118800	2.49767673	0.02533184
261000	2.43346108	0.04430479	172800	2.43027911	0.03638582
280800	2.46702794	0.04631361	190800	2.28611139	0.04071384
360000	2.47706022	0.06045419	-	-	-

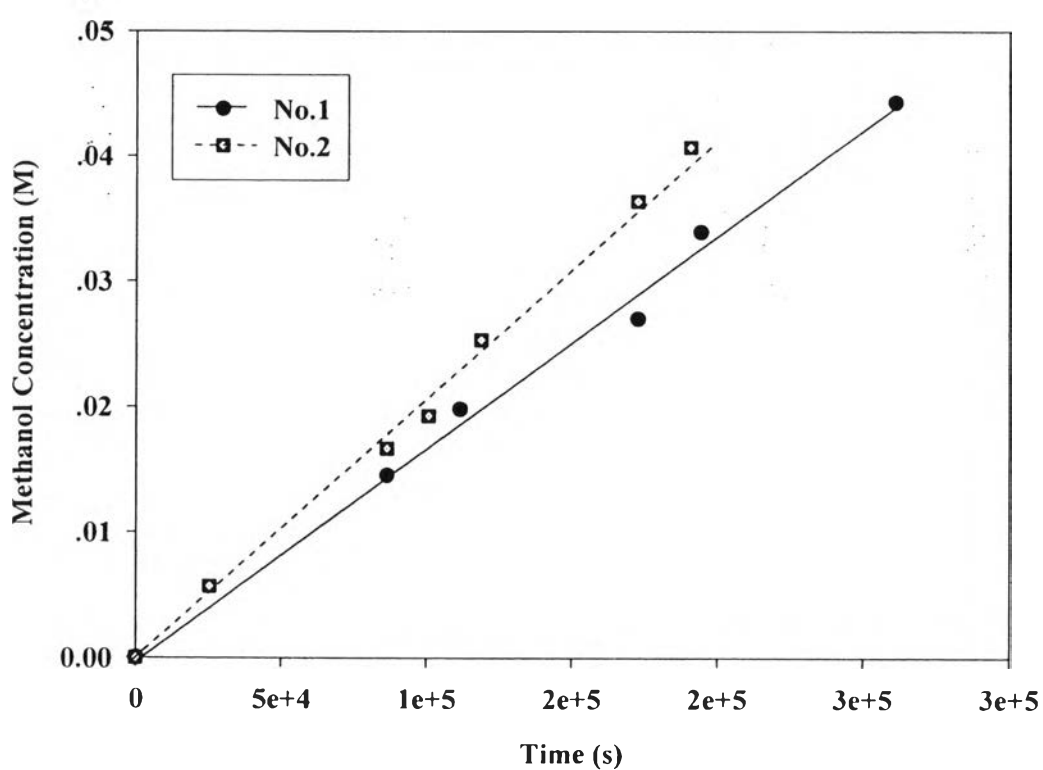
**Figure C4** Methanol concentration (M) in compartment B vs. time (s) of S-coPI-1.

Table C5 Raw data of methanol permeability calculation of S-coPI-2

No.1 Thickness 181.00 μm			No.2 Thickness 126.75 μm		
Time (second)	MeOH concentration (M)		Time (second)	MeOH concentration (M)	
	Comp. A	Comp. B		Comp. A	Comp. B
0	2.499460951	0	0	2.41380186	0
27000	2.495410412	0.004203517	14400	2.50578163	0.00474034
86400	2.458800783	0.017110451	24300	2.50876770	0.00889070
100800	2.482017954	0.019234386	82800	2.51359824	0.02617540
120600	2.469973536	0.024151167	100800	2.42515345	0.03156249
173700	2.471091453	0.033369331	165600	2.41709345	0.04879925
190800	2.426317034	0.035984344	180000	2.40864570	0.05184493

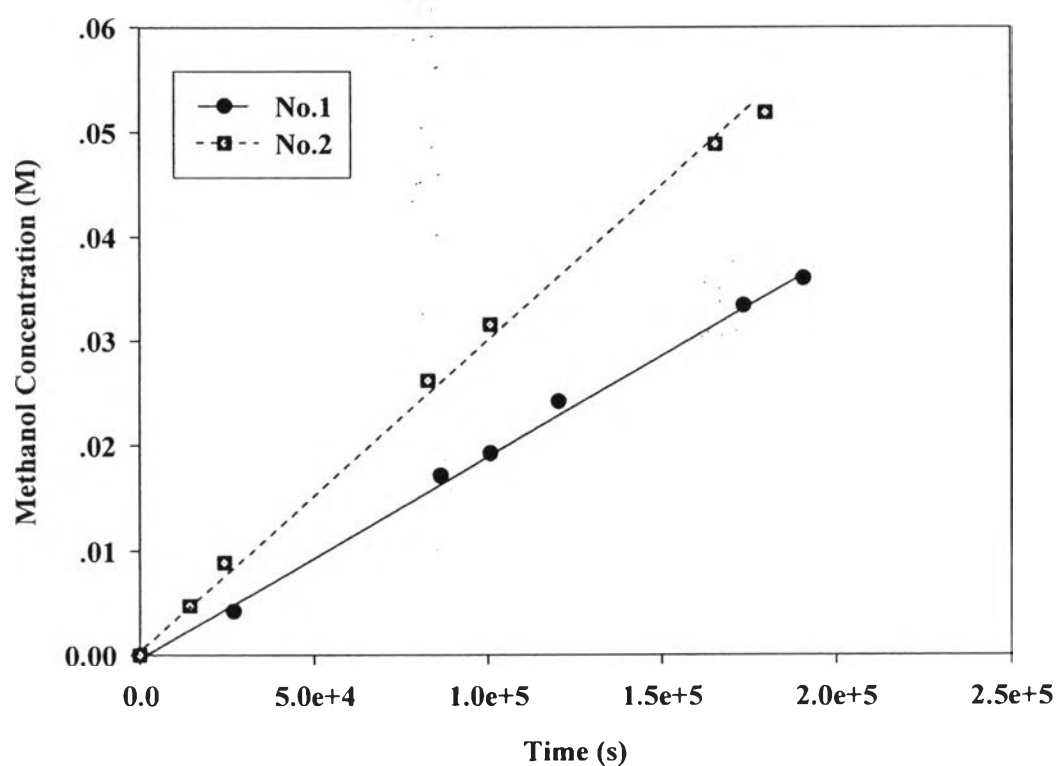
**Figure C5** Methanol concentration (M) in compartment B vs. time (s) of S-coPI-2.

Table C6 Raw data of methanol permeability calculation of S-coPI-3

No.1 Thickness 187.83 μm			No.2 Thickness 150.83 μm		
Time (second)	MeOH concentration (M)		Time (second)	MeOH concentration (M)	
	Comp. A	Comp. B		Comp. A	Comp. B
0	2.50511	0	0	2.504947	0
32400	2.481517	0.00306255	14400	2.451174	0.00120023
81000	2.467978	0.00782958	100800	2.513047	0.01153467
100800	2.423779	0.01018472	118800	2.420381	0.0135183
160200	2.372493	0.01753651	158400	2.461952	0.01966417
198000	2.446137	0.02065207	180000	2.405483	0.02196294
-	-	-	196200	2.400274	0.02308328

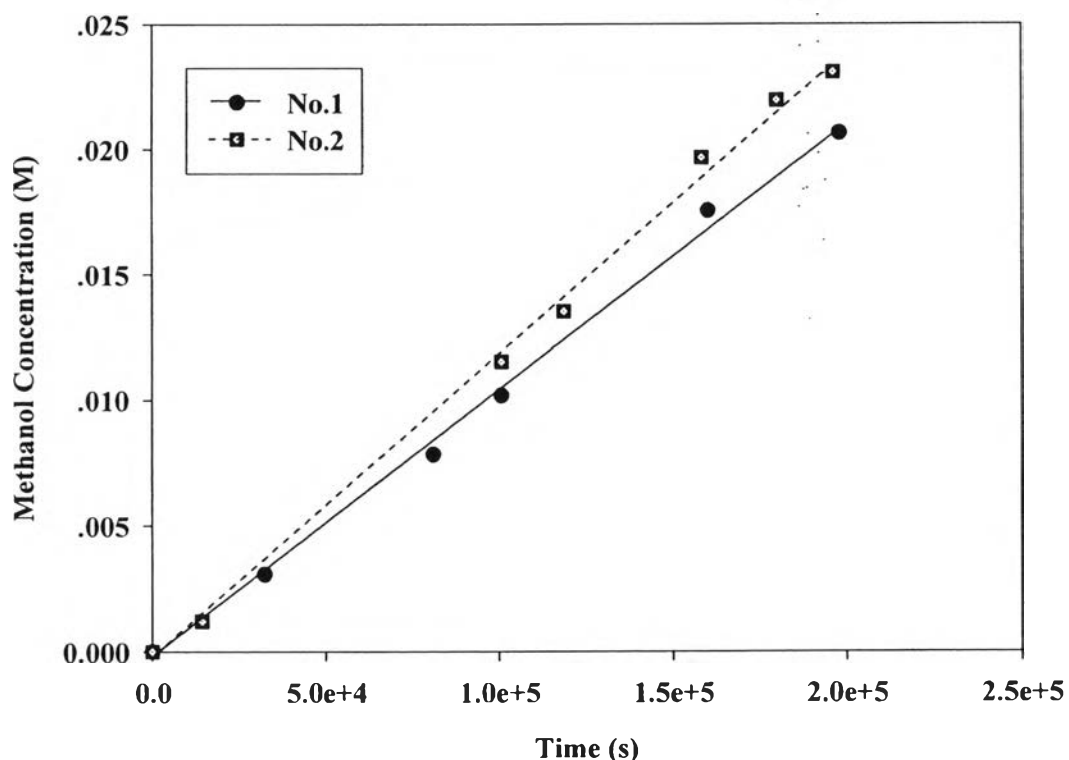
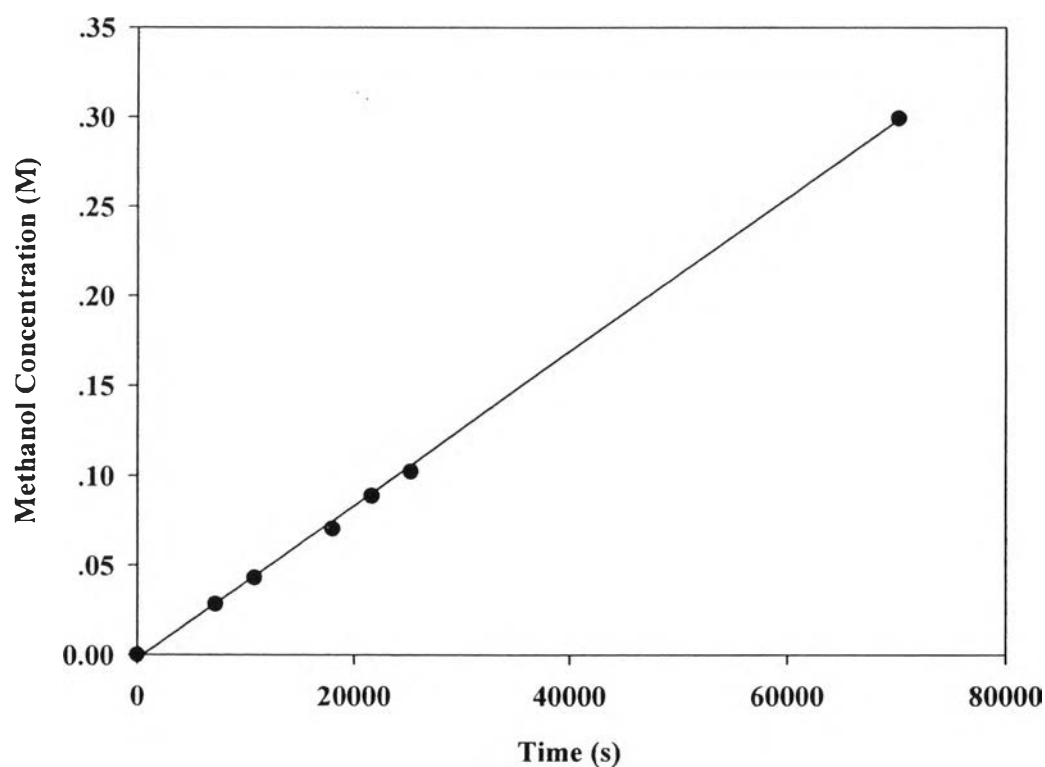
**Figure C6** Methanol concentration (M) in compartment B vs. time (s) of S-coPI-3.

Table C7 Raw data of methanol permeability calculation of Nafion117

Thickness 200.83 μm		
Time (second)	MeOH concentration (M)	
	Comp. A	Comp. B
0	2.502839511	0
7200	2.429209137	0.02819362
10800	2.386751582	0.043030645
18000	2.300717399	0.070503426
21600	2.361906431	0.088747749
25200	2.207041532	0.102298469
70200	2.194559572	0.299236676
86400	2.177379724	0.34028372

**Figure C7** Methanol concentration (M) in compartment B vs. time (s) of Nafion117.

Appendix D Tensile Test

The mechanical properties of the polymer films were measured using a universal testing machine (Lloyd, model SMT2-500N) at the gauge length 30.0 mm, at the speed of 10mm/min, and at room temperature. At least five measurements were taken for each polymer sample. The membranes about 160 - 200 μm in thickness were cut in to 1 cm \times 5 cm pieces and soaked in a deionized water for 2 days before testing.

Table D1 Tensile test results of S-coPI and Nafion117 membranes

Sample No.	Thickness (μm)	Young's modulus (MPa)	Tensile strength (MPa)	Elongation at break (%)
Non S-coPI	184 ± 11.40	651.00 ± 53.84	28.44 ± 2.17	10.18 ± 0.65
S-coPI-1	188 ± 17.89	829.58 ± 27.84	35.83 ± 1.48	10.76 ± 0.80
S-coPI-2	180 ± 12.25	980.01 ± 68.88	43.63 ± 3.37	11.93 ± 1.56
S-coPI-3	174 ± 19.49	1065.10 ± 47.86	47.67 ± 3.38	8.64 ± 0.42
Nafion117*	-	100	28.4	329.2

*Liu *et al.*, 2007

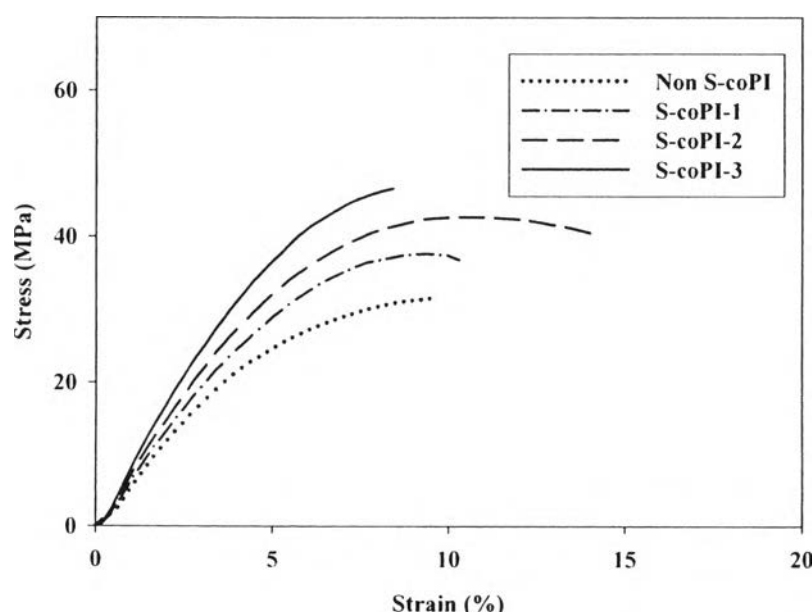


Figure D1 Stress-strain behaviour of S-coPI membranes.

Table D2 Tensile test results of Non S-coPI membranes

Sample No.	Thickness (μm)	Young's modulus (MPa)	Tensile strength (MPa)	Elongation at break (%)
1	200	657.34	26.871	9.83
2	190	726.66	31.758	9.96
3	180	665.74	28.915	9.45
4	180	580.65	26.183	11.09
5	170	625.22	28.464	10.57
Average	184 ± 11.40	651.00 ± 53.84	28.44 ± 2.17	10.18 ± 0.65

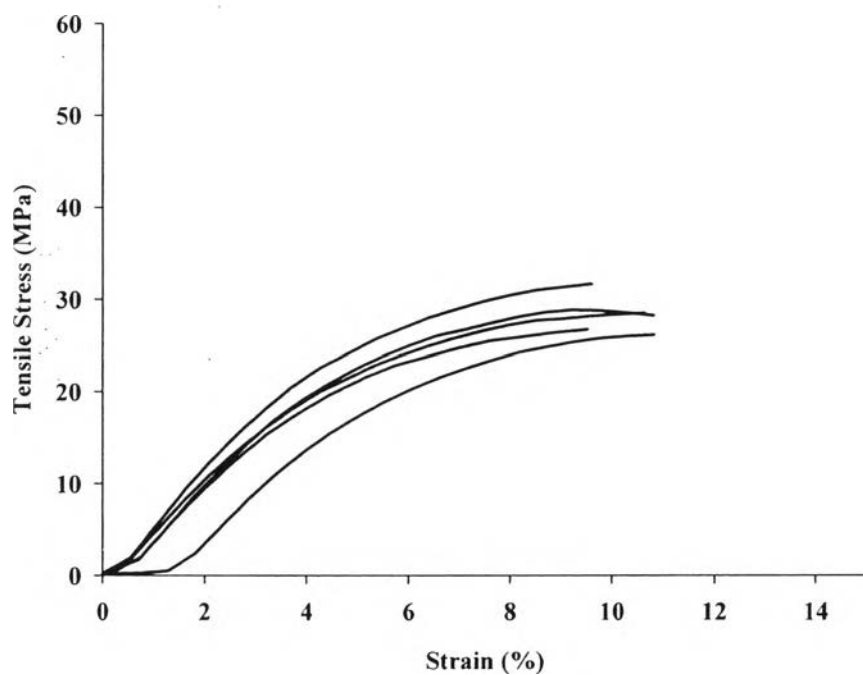
**Figure D2** Stress-strain behaviour of Non S-coPI membranes.

Table D3 Tensile test results of S-coPI-1 membranes

Sample No.	Thickness (μm)	Young's modulus (MPa)	Tensile strength (MPa)	Elongation at break (%)
1	200	841.75	37.65	10.29
2	200	835.82	36.94	11.59
3	200	783.46	35.77	11.57
4	160	857.63	34.61	9.79
5	180	829.23	34.18	10.57
Average	188 ± 17.89	829.58 ± 27.84	35.83 ± 1.48	10.76 ± 0.80

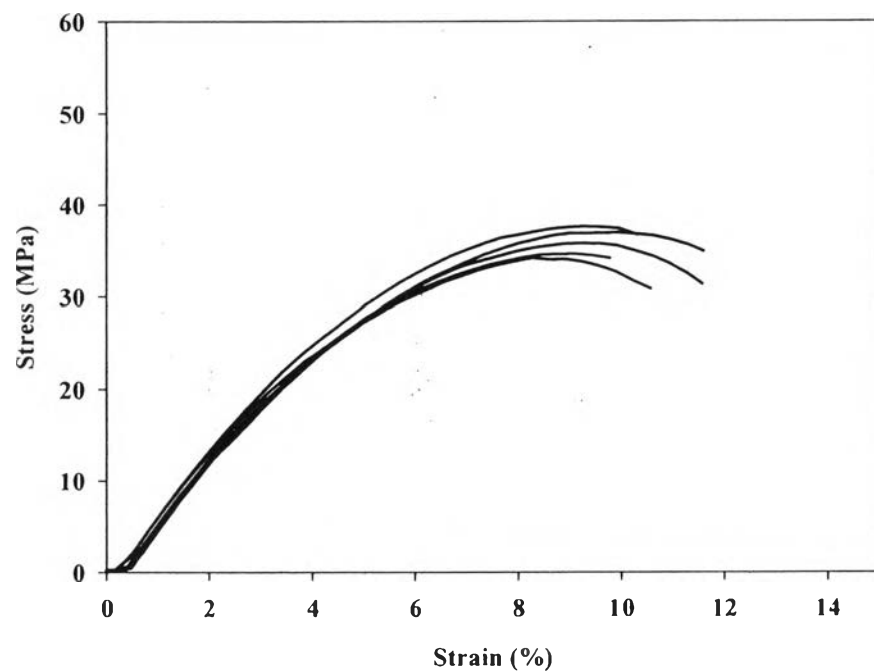
**Figure D3** Stress-strain behaviour of S-coPI-3 membranes.

Table D4 Tensile test results of S-coPI-2 membranes

Sample No.	Thickness (μm)	Young's modulus (MPa)	Tensile strength (MPa)	Elongation at break (%)
1	180	990.66	45.714	12.25
2	160	980.75	42.621	13.91
3	190	904.14	40.352	12.78
4	190	937.99	41.053	10.12
5	180	1086.5	48.388	10.61
Average	180 ± 12.25	980.01 ± 68.88	43.63 ± 3.37	11.93 ± 1.56

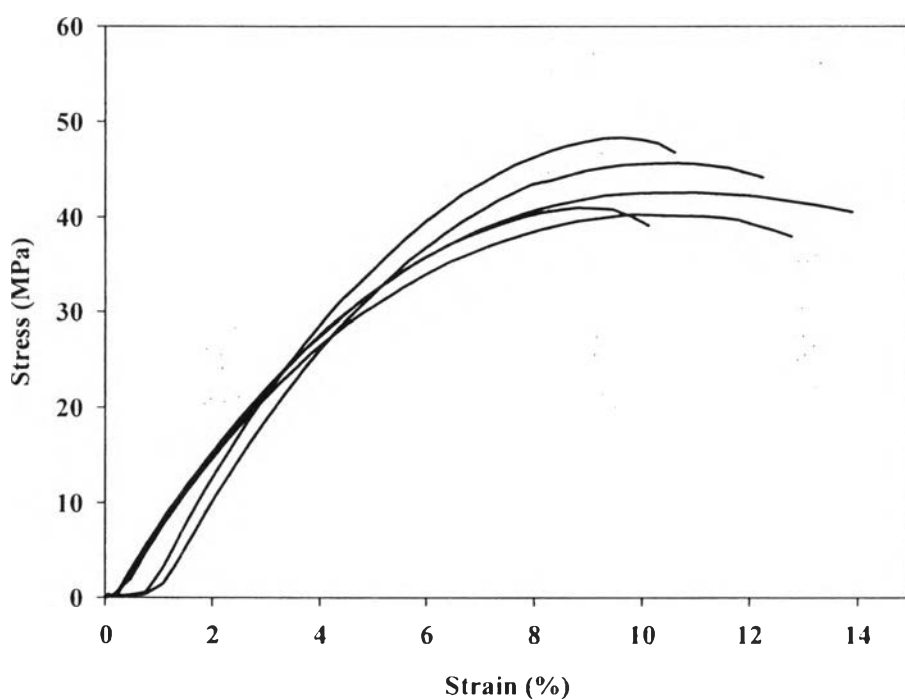
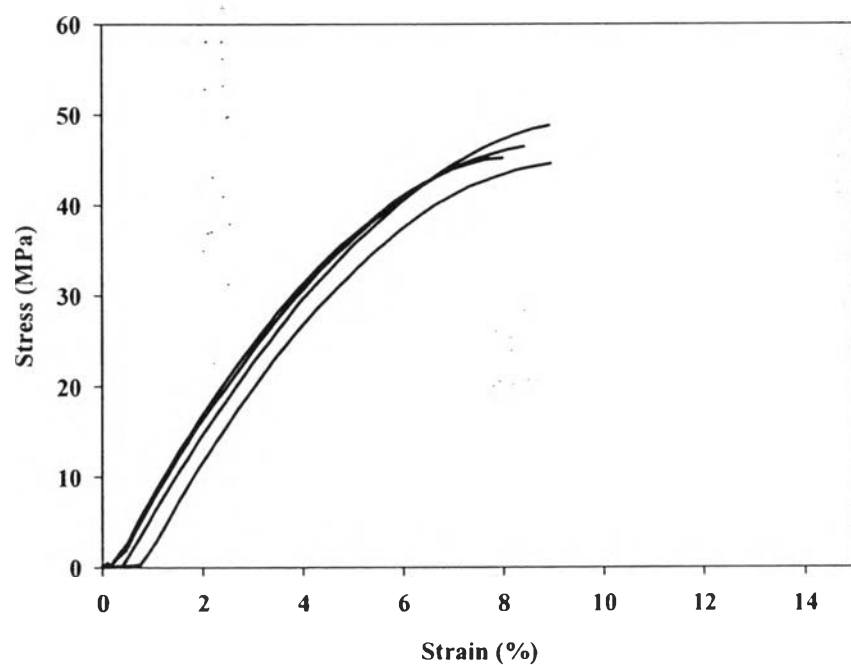
**Figure D4** Stress-strain behaviour of S-coPI-2 membranes.

Table D5 Tensile test results of S-coPI-3 membranes

Sample No.	Thickness (μm)	Young's modulus (MPa)	Tensile strength (MPa)	Elongation at break (%)
1	200	1013.6	48.837	8.9199
2	190	1118.6	52.989	8.9199
3	160	1109.6	46.628	8.4175
4	160	1059	45.323	7.996
5	160	1024.7	44.584	8.9457
Average	174 ± 19.49	1065.10 ± 47.86	47.67 ± 3.38	8.64 ± 0.42

**Figure D5** Stress-strain behaviour of S-coPI-3 membranes.

Appendix E Water Uptake and Moisture Absorption

The polymer membranes were dried in an oven at 100 °C for 24 h. The dried membranes were weighed (W_d). Then the polymers were soaked in de-ionized water at a room temperature for 2 days. They were removed from the water, quickly dry-wiped with an absorbent paper to remove any surface moisture, and then weighed immediately to determine their wet masses (W_w). The measurements were repeated three times to obtain the average water uptake value. The water uptake was calculated with the following formula (E1):

$$\text{Water uptake}(\%) = \frac{(W_w - W_d) \times 100}{W_d} \quad (\text{E1})$$

The moisture absorption was determined in the same method of the water uptake but after the membranes were dried, the membranes were placed at a room temperature for 2 days before weighted (W_m) again. The moisture absorption was calculated with the following formula (E2):

$$\text{Moisture absorption}(\%) = \frac{(W_m - W_d) \times 100}{W_d} \quad (\text{E1})$$

Table E1 The Water uptake and moisture absorption of S-coPI and Nafion117 films

Sample	Water uptake (%)	Moisture absorption (%)
Non S-coPI	8.367 ± 0.219	4.268 ± 0.247
S-coPI-1	7.778 ± 0.462	3.501 ± 0.601
S-coPI-2	8.134 ± 0.270	4.149 ± 0.468
S-coPI-3	11.173 ± 0.252	5.091 ± 0.185
Nafion117	20.525 ± 0.028	3.499 ± 0.198

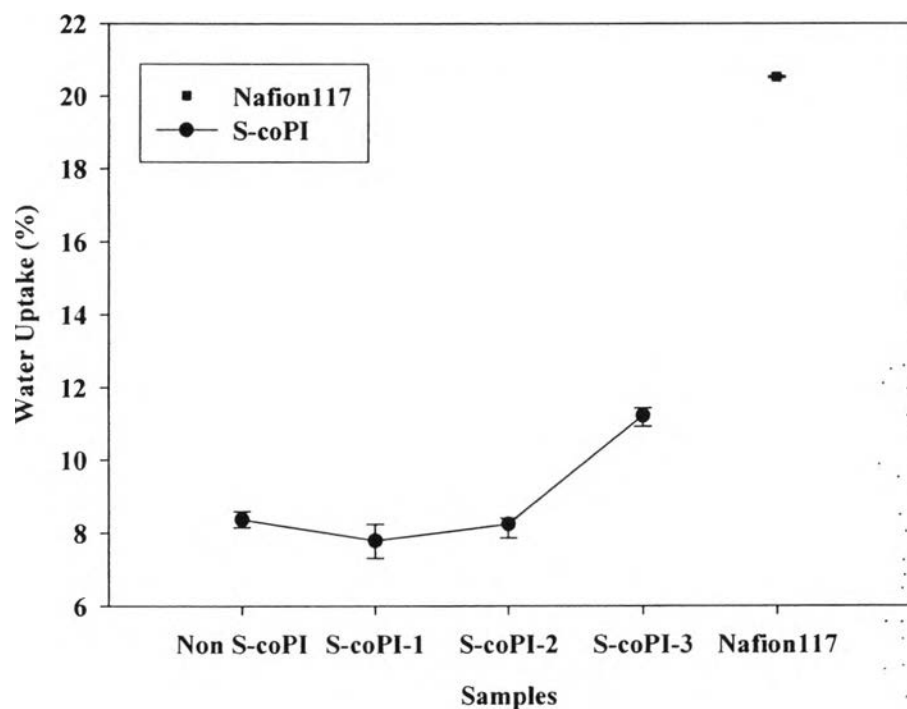


Figure E1 Water uptake of S-coPI and Nafion117 films.

Table E2 Raw data of water uptake calculations

Sample	No.	Wet (mg)	Dry (mg)	Water (mg)	Water uptake (%)
Non S-coPI	1	25.9	23.9	2.0	8.36820
	2	29.2	27.0	2.2	8.14814
	3	21.5	19.8	1.7	8.58586
S-coPI-1	1	17.1	15.8	1.3	8.22785
	2	19.1	17.8	1.3	7.30337
	3	16.6	15.4	1.2	7.79221
S-coPI-2	1	24.8	23.0	1.8	7.82609
	2	19.7	18.2	1.5	8.24176
	3	20.8	19.2	1.6	8.33333
S-coPI-3	1	23.4	21.1	2.3	10.9005
	2	22.8	20.5	2.3	11.2195
	3	21.5	19.3	2.2	11.3989
Nafion117	1	78.1	64.8	13.3	20.5246
	2	78.6	65.2	13.4	20.5521
	3	77.6	64.4	13.2	20.4968

Table E3 Raw data of moisture absorption calculations

Sample	No.	T_{room} (mg)	Dry (mg)	Water (mg)	Water uptake (%)
Non S-coPI	1	24.9	23.9	1.0	4.1841
	2	28.1	27.0	1.1	4.0741
	3	20.7	19.8	0.9	4.5454
S-coPI-1	1	16.4	15.8	0.6	3.7975
	2	18.3	17.8	0.5	2.8089
	3	16.0	15.4	0.6	3.8961
S-coPI-2	1	23.9	23.0	0.9	3.9130
	2	18.9	18.2	0.7	3.8461
	3	20.1	19.2	0.9	4.6875
S-coPI-3	1	22.2	21.1	1.1	5.2133
	2	21.5	20.5	1.0	4.8780
	3	20.3	19.3	1.0	5.1813
Nafion117	1	67.0	64.8	2.2	3.3951
	2	67.4	65.2	2.2	3.3742
	3	66.8	64.4	2.4	3.7267

Appendix F Determination of Proton Conductivity

Proton conductivity of the films was measured by an Agilent E4980A LCR meter in terms of the impedance data. The fully hydrated films (immersed in deionized water for 2 days) were cut into 0.5×0.5 cm pieces and painted with a silver paint on both sides of the films. The films were measured at a potential of 1 V and an alternating current with the frequency range of 20 Hz - 2 MHz. Then data were plotted between Z' and Z'' . The conductivity σ of the samples was calculated from the impedance data by the following equation;

$$\sigma(S \text{ cm}^{-1}) = \frac{d}{SR} \quad (\text{F1})$$

where σ = proton conductivity

d = thickness of the membrane

S = the area of the interface between the membrane and the electrode

R = the measured resistance of the membrane – derived from the intersection of the low frequency semi-circle on the complex impedance plane with the Z' axis.

Table F1 The proton conductivity of Non S-coPI and S-coPI membranes

Sample	Proton Conductivity ($S \text{ cm}^{-1}$)		
	no.1	no.2	Average
Non S-coPI	4.48×10^{-10}	5.66×10^{-10}	5.07×10^{-10}
S-coPI-1	1.41×10^{-8}	1.06×10^{-7}	6.01×10^{-8}
S-coPI-2	1.85×10^{-3}	1.61×10^{-3}	1.73×10^{-3}
S-coPI-3	1.11×10^{-2}	1.21×10^{-2}	1.16×10^{-2}

Table F2 Raw data of proton conductivity calculations

Sample	Thickness (cm)	Area (cm ²)	R (ohms)	Conduct (S cm ⁻¹)
Non S-coPI	0.026767	0.070714286	845000000	4.47951×10^{-10}
	0.019817	0.070714286	495000000	5.66134×10^{-10}
S-coPI-1	0.019933	0.070714286	2000000	1.40943×10^{-8}
	0.014967	0.070714286	2000000	1.05825×10^{-7}
S-coPI-2	0.024233	0.070714286	185	1.85240×10^{-3}
	0.024267	0.070714286	213.3	1.60884×10^{-3}
S-coPI-3	0.018167	0.070714286	23.22	1.10640×10^{-2}
	0.023300	0.070714286	27.33	1.20562×10^{-2}

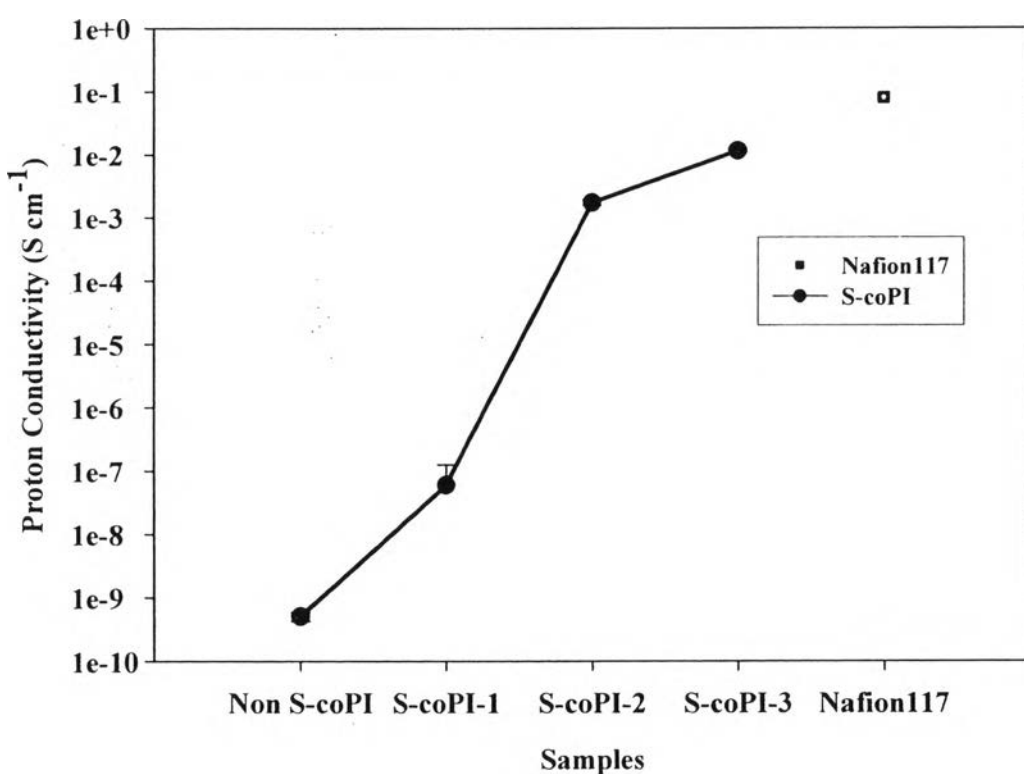
**Figure F1** The proton conductivity of and the S-coPI and Nafion117 films..

Table F3 Proton conductivity raw data of Non S-coPI film

Frequency, Hz	$Z(10^6)$, ohm	θ , degree	r, Radius	$Z' = Z \cos \theta$	$Z'' = Z \sin \theta$
20	624.066	-19.9473	-0.348158	5.87E+08	-2.13E+08
40	529.496	-26.6371	-0.464921	4.73E+08	-2.37E+08
60	454.893	-32.0577	-0.5595315	3.86E+08	-2.41E+08
70	418.494	-34.2018	-0.5969544	3.46E+08	-2.35E+08
80	385.897	-36.8876	-0.6438321	3.09E+08	-2.32E+08
150	280.888	-46.136	-0.8052526	1.95E+08	-2.03E+08
200	236.218	-49.6981	-0.8674251	1.53E+08	-1.80E+08
400	147.818	-57.431	-1.0023943	7.96E+07	-1.25E+08
600	109.128	-59.7091	-1.042156	5.50E+07	-9.42E+07
800	88.5599	-60.8933	-1.0628249	4.31E+07	-7.74E+07
1500	55.3957	-62.7847	-1.0958372	2.53E+07	-4.93E+07
2000	44.7716	-63.1995	-1.1030771	2.02E+07	-4.00E+07
4000	26.5671	-64.2066	-1.1206549	1.16E+07	-2.39E+07
6000	20.0167	-64.7196	-1.1296087	8.55E+06	-1.81E+07
8000	16.3	-65.5601	-1.1442787	6.74E+06	-1.48E+07
20000	8.19351	-69.5236	-1.2134572	2.87E+06	-7.68E+06
40000	4.71219	-72.2555	-1.2611395	1.44E+06	-4.49E+06
60000	3.37299	-73.8167	-1.2883885	9.40E+05	-3.24E+06
80000	2.64441	-74.8033	-1.3056085	6.93E+05	-2.55E+06
200000	1.20779	-78.4692	-1.3695927	2.41E+05	-1.18E+06
400000	0.656202	-81.3784	-1.4203696	9.83E+04	-6.49E+05

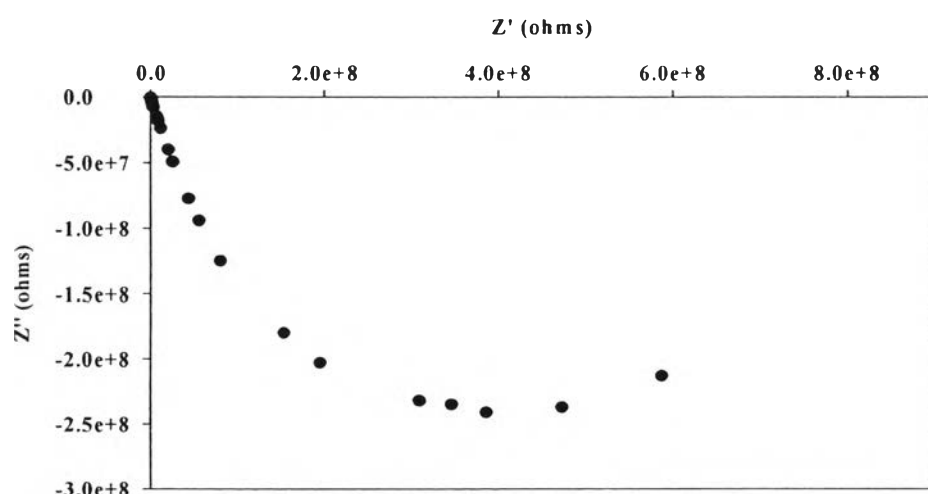
**Figure F2** Nyquist plot of the Non S-coPI membrane.

Table F4 Proton conductivity raw data of Non S-coPI film

Frequency, Hz	$Z(10^6)$, ohm	θ , degree	r, Radius	$Z' = Z \cos \theta$	$Z'' = Z \sin \theta$
20	422.619	-55.222	-0.9638387	2.41E+08	-3.47E+08
40	282.251	-51.8081	-0.9042528	1.75E+08	-2.22E+08
60	227.152	-37.4474	-0.6536028	1.80E+08	-1.38E+08
70	213.035	-35.4134	-0.6181015	1.74E+08	-1.23E+08
80	207.4433	-37.3822	-0.6524648	1.65E+08	-1.26E+08
150	151.214	-48.0372	-0.838436	1.01E+08	-1.12E+08
200	131.301	-50.6591	-0.8841983	8.32E+07	-1.02E+08
400	90.8722	-54.3176	-0.9480534	5.30E+07	-7.38E+07
600	71.8308	-57.1935	-0.998249	3.89E+07	-6.04E+07
800	59.8875	-59.8492	-1.0446013	3.01E+07	-5.18E+07
1500	38.5979	-65.1958	-1.1379202	1.62E+07	-3.50E+07
2000	31.2065	-67.6127	-1.1801046	1.19E+07	-2.89E+07
4000	17.8669	-72.677	-1.2684963	5.32E+06	-1.71E+07
6000	12.7291	-74.9821	-1.3087292	3.30E+06	-1.23E+07
8000	9.99419	-76.5781	-1.3365856	2.32E+06	-9.72E+06
20000	4.41681	-80.6549	-1.4077417	7.17E+05	-4.36E+06
40000	2.32785	-82.6776	-1.4430456	2.97E+05	-2.31E+06
60000	1.58873	-83.5588	-1.458426	1.78E+05	-1.58E+06
80000	1.22845	-83.9835	-1.4658387	1.29E+05	-1.22E+06
200000	0.5139	-85.0736	-1.4848652	4.41E+04	-5.12E+05
400000	0.266283	-85.5993	-1.4940407	2.04E+04	-2.65E+05

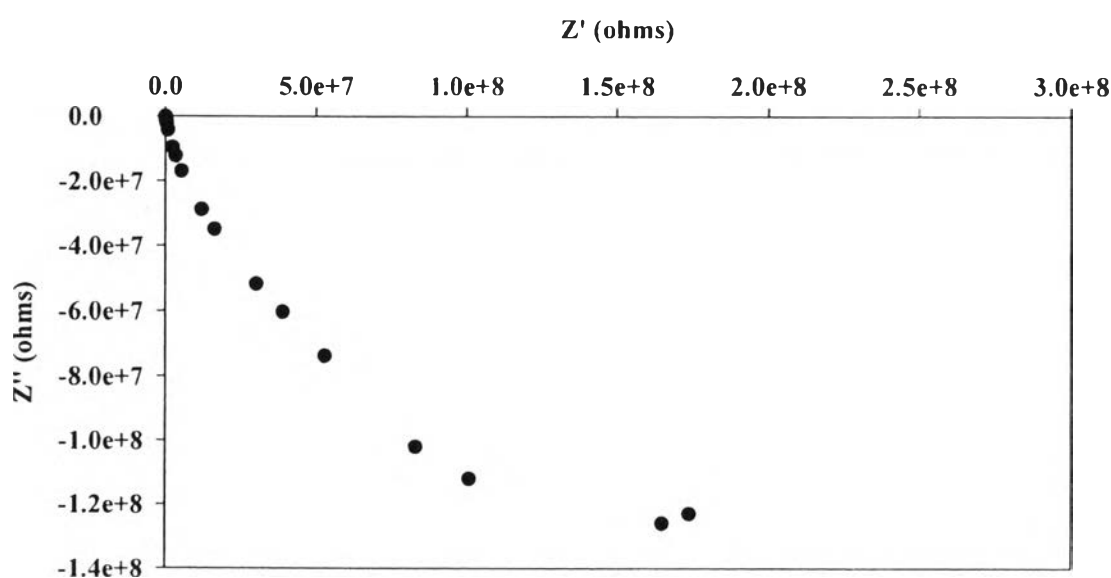
**Figure F3** Nyquist plot of the Non S-coPI membrane.

Table F5 Proton conductivity raw data of S-coPI-1 film

Frequency, Hz	$Z(10^6)$, ohm	r, Radius	$Z' = Z \cos \theta$	$Z'' = Z \sin \theta$
600	18.2364	-349.175	1.71E+07	-6.24E+06
800	17.6301	-383.135	1.64E+07	-6.59E+06
1500	15.5794	-517.34	1.35E+07	-7.71E+06
2000	14.1361	-602.373	1.16E+07	-8.01E+06
4000	10.4525	-860.246	6.82E+06	-7.92E+06
6000	8.05525	-1009.71	4.29E+06	-6.82E+06
8000	6.58051	-1115.6	2.89E+06	-5.91E+06
20000	3.00568	-1303.85	7.93E+05	-2.90E+06
40000	1.61166	-1358.39	3.40E+05	-1.58E+06
60000	1.12512	-1399.12	1.92E+05	-1.11E+06
80000	0.868728	-1396.79	1.50E+05	-8.56E+05
200000	0.402614	-1256.89	1.24E+05	-3.83E+05
400000	0.322829	-1145.61	1.33E+05	-2.94E+05
800000	0.063371	-1204.87	2.27E+04	-5.92E+04
2000000	0.026316	-1368.42	5.29E+03	-2.58E+04

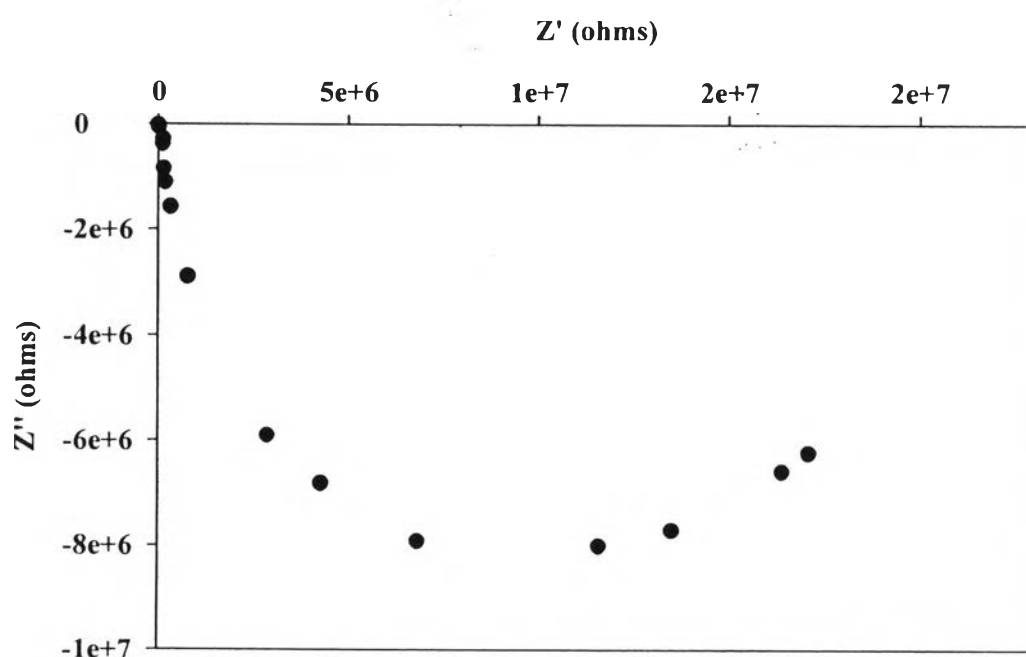
**Figure F4** Nyquist plot of the S-coPI-1 membrane.

Table F6 Proton conductivity raw data of S-coPI-1 film

Frequency, Hz	$Z(10^6)$, ohm	r, Radius	$Z' = Z \cos r$	$Z'' = Z \sin r$
2000	1.72379	-297.451	1.65E+06	-5.05E+05
4000	1.57333	-393.501	1.45E+06	-6.03E+05
6000	1.49221	-454.83	1.34E+06	-6.56E+05
8000	1.31343	-543.405	1.12E+06	-6.79E+05
20000	0.895521	-773.515	6.41E+05	-6.26E+05
40000	0.582558	-911.05	3.57E+05	-4.60E+05
60000	0.457174	-983.104	2.53E+05	-3.80E+05
80000	0.375313	-1027.69	1.94E+05	-3.21E+05
200000	0.202614	-1133.15	8.59E+04	-1.84E+05
400000	0.122829	-1165.97	4.84E+04	-1.13E+05
800000	0.073371	-1200.34	2.66E+04	-6.84E+04
2000000	0.036316	-1269.7	1.08E+04	-3.47E+04

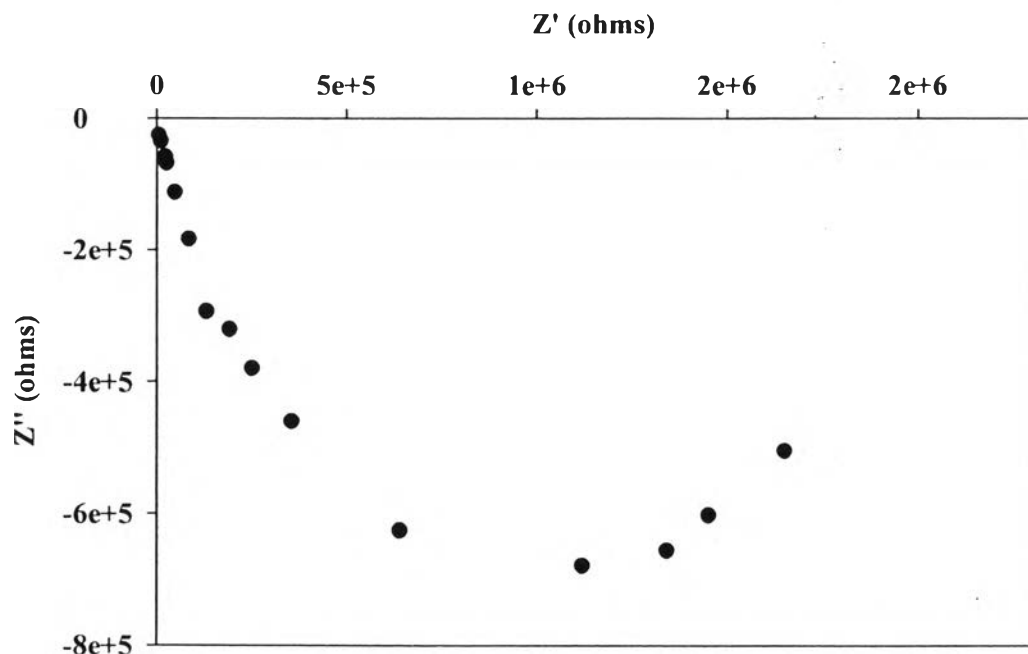
**Figure F5** Nyquist plot of the S-coPI-1 membrane.

Table F7 Proton conductivity raw data of S-coPI-2 film

Frequency, Hz	Z, ohm	r, Radius	Z'=Zcosr	Z''=Zsinr
20	184.518	-26.3343	1.85E+02	-4.86E-03
40	184.473	41.375	1.84E+02	7.63E-03
50	184.313	80.4786	1.84E+02	1.48E-02
70	184.174	98.929	1.84E+02	1.82E-02
80	183.857	147.624	1.84E+02	2.71E-02
100	183.69	158.727	1.84E+02	2.92E-02
120	183.479	167.664	1.83E+02	3.08E-02
150	183.135	181.636	1.83E+02	3.33E-02
500	182.664	170.883	1.83E+02	3.12E-02
600	182.529	158.141	1.83E+02	2.89E-02
700	182.295	146.022	1.82E+02	2.66E-02
800	182.256	135.847	1.82E+02	2.48E-02
1200	182.038	110.812	1.82E+02	2.02E-02

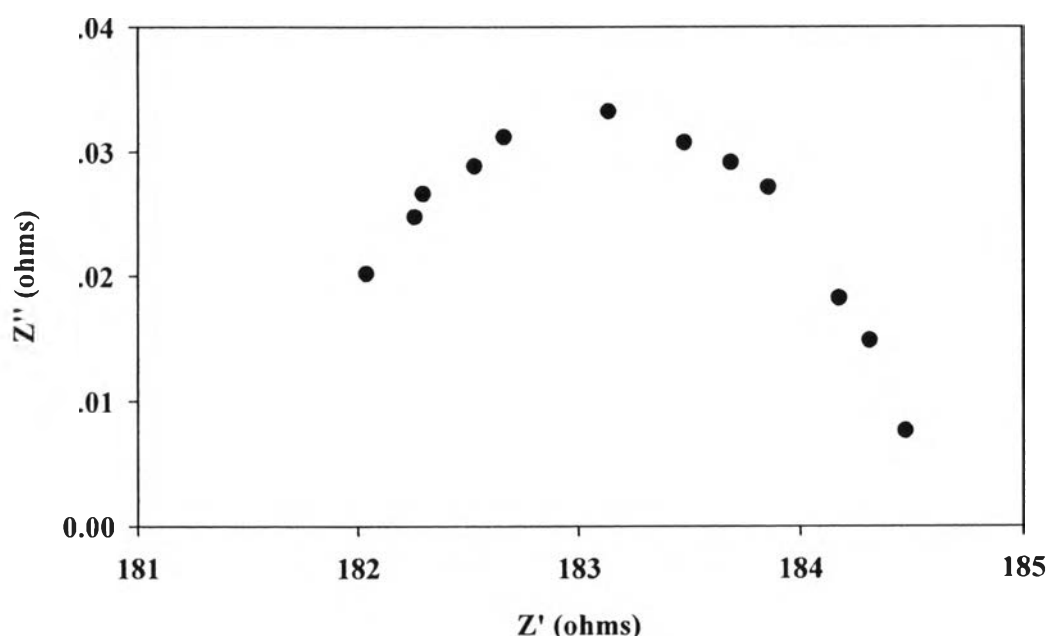
**Figure F6** Nyquist plot of the S-coPI-2 membrane.

Table F8 Proton conductivity raw data of S-coPI-2 film

Frequency, Hz	Z, ohm	r, Radius	Z'=Zcosr	Z''=Zsinr
20	213.594	-89.9921	2.14E+02	-1.92E-02
30	213.336	13.212	2.13E+02	2.82E-03
40	213.01	61.714	2.13E+02	1.31E-02
50	212.833	106.281	2.13E+02	2.26E-02
60	212.194	143.06	2.12E+02	3.04E-02
70	211.955	176.702	2.12E+02	3.75E-02
80	211.855	201.215	2.12E+02	4.26E-02
100	211.334	220.605	2.11E+02	4.66E-02
500	210.141	231.961	2.10E+02	4.87E-02
600	209.98	248.756	2.10E+02	5.22E-02
700	209.218	240.407	2.09E+02	5.03E-02
800	208.633	250.02	2.09E+02	5.22E-02
1200	207.379	217.493	2.07E+02	4.51E-02

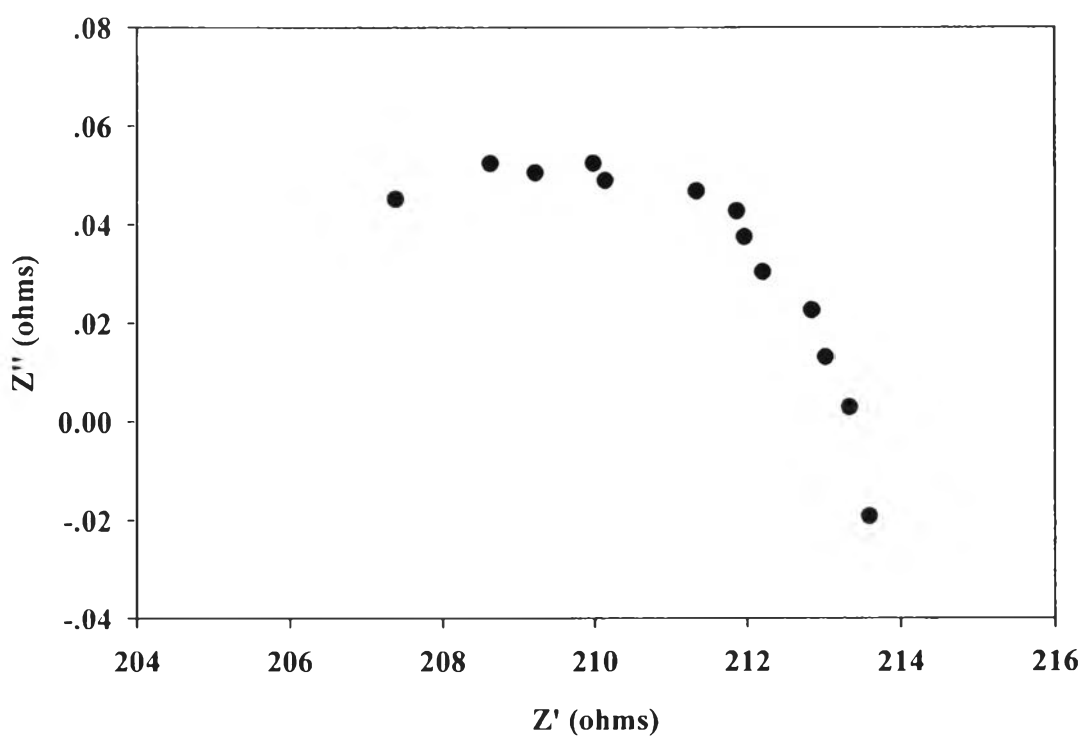
**Figure F7** Nyquist plot of the S-coPI-2 membrane.

Table F9 Proton conductivity raw data of S-coPI-3 film

Frequency, Hz	Z, ohm	r, Radius	Z'=Zcosr	Z''=Zsinr
120	27.293	13.9169	2.73E+01	3.80E-04
140	27.1148	65.018	2.71E+01	1.76E-03
150	26.783	87.9159	2.68E+01	2.35E-03
160	26.342	94.8511	2.63E+01	2.50E-03
170	26.169	88.6188	2.62E+01	2.32E-03
180	26.0332	80.1256	2.60E+01	2.09E-03
200	25.9006	75.9692	2.59E+01	1.97E-03
250	25.7242	58.2141	2.57E+01	1.50E-03
300	25.5984	47.4546	2.56E+01	1.21E-03
400	25.4643	26.5109	2.55E+01	6.75E-04
500	25.4053	15.9183	2.54E+01	4.04E-04
600	25.3882	6.89512	2.54E+01	1.75E-04

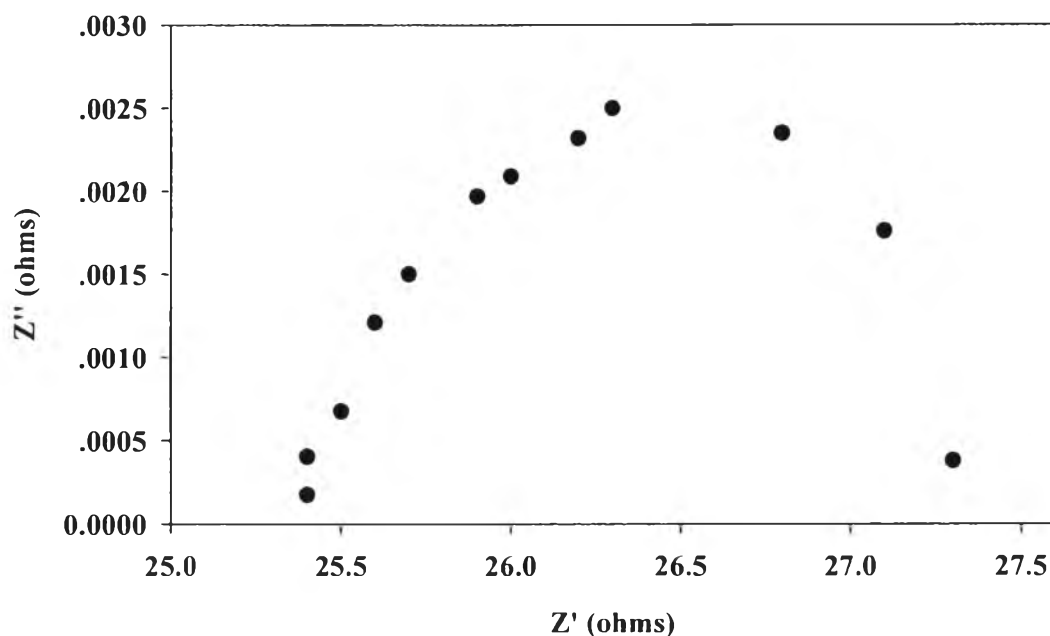
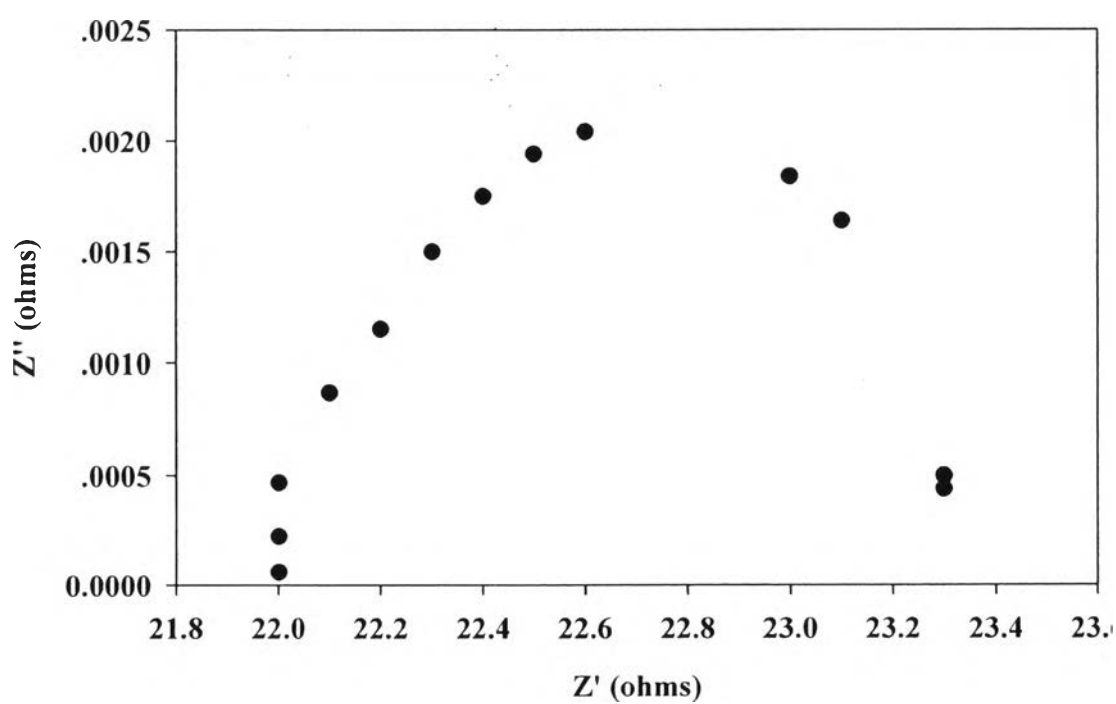
**Figure F8** Nyquist plot of the S-coPI-3 membrane.

Table F10 Proton conductivity raw data of S-coPI-3 film

Frequency, Hz	Z, ohm	r, Radius	Z'=Zcosr	Z''=Zsinr
110	23.3131	18.7128	2.33E+01	4.36E-04
120	23.2909	21.2667	2.33E+01	4.95E-04
140	23.1261	70.7905	2.31E+01	1.64E-03
150	23.0191	79.7906	2.30E+01	1.84E-03
160	22.588	90.3542	2.26E+01	2.04E-03
170	22.4721	86.5161	2.25E+01	1.94E-03
180	22.3685	78.4426	2.24E+01	1.75E-03
200	22.302	67.2836	2.23E+01	1.50E-03
250	22.1882	51.6313	2.22E+01	1.15E-03
300	22.1323	39.1974	2.21E+01	8.68E-04
400	22.0353	21.1372	2.20E+01	4.66E-04
500	22.0139	10.174	2.20E+01	2.24E-04
600	22.0085	2.6426	2.20E+01	5.82E-05

**Figure F9** Nyquist plot of the S-coPI-3 membrane.

Appendix G $^1\text{H-NMR}$

$^1\text{H-NMR}$ spectrum of 4,4'-diaminodiphenyl methane (DDM) and 4,4'-diaminodiphenyl methane-2,2'-disulfonic acid disodium salt (S-DDM) in deuterated dimethylsulfoxide (DMSO-d_6) were measured on a Varian mercury 400 MHz. The degree of sulfonation was determined by integration of distinct aromatic signals (Javaid Zaidi, 2003).

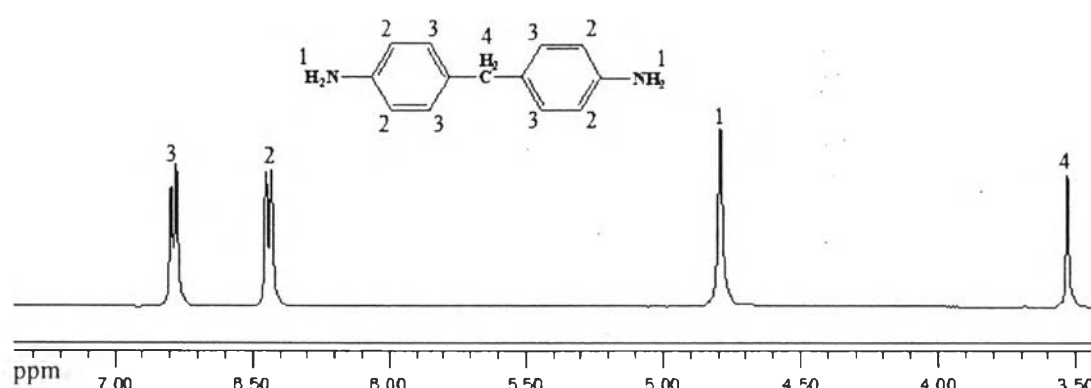


Figure G1 The $^1\text{H-NMR}$ spectrum of DDM

Figure G1 shows the $^1\text{H-NMR}$ spectrum of DDM, the signal at 6.78 ppm (doublet) and 6.44 ppm (doublet) are assigned to the aromatic proton H_3 and H_2 , respectively. The signal at 4.79 ppm (singlet) is assigned to the primary anime proton H_1 and the signal at 3.53 ppm (singlet) is attributed to the methylene proton H_4 .

The $^1\text{H-NMR}$ of S-DDM peak is shown in the Figure G2. The signal at 7.16 ppm (doublet), 7.12 ppm (doublet of singlet), and 6.71 ppm (doublet of doublet) are attributed to the aromatic protons H_3 , H_5 , and H_2 , respectively. The signal at 5.55 ppm (singlet) is assigned the primary anime proton, correlated with H_1 . The signal at 3.82 ppm (singlet) is assigned to the methylene proton H_4 between the phenyl groups.

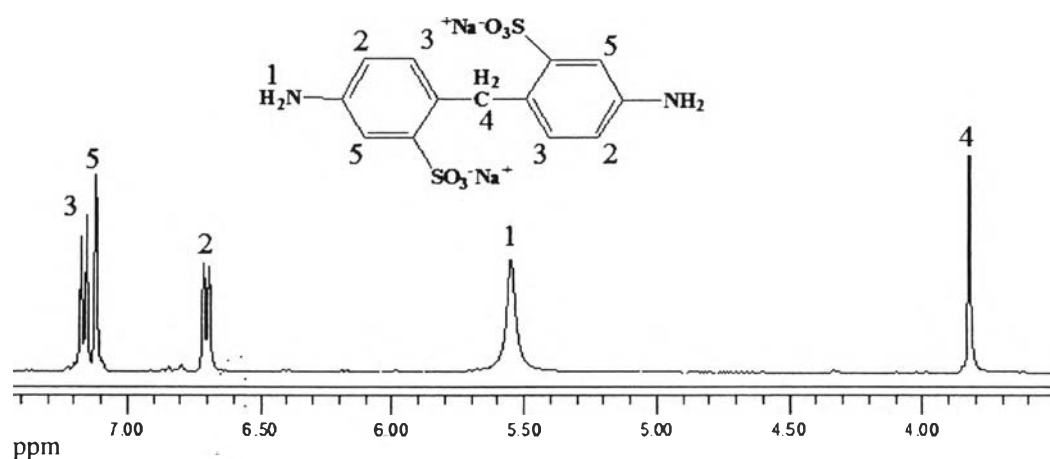


Figure G2 The ^1H -NMR spectrum of S-DDM.

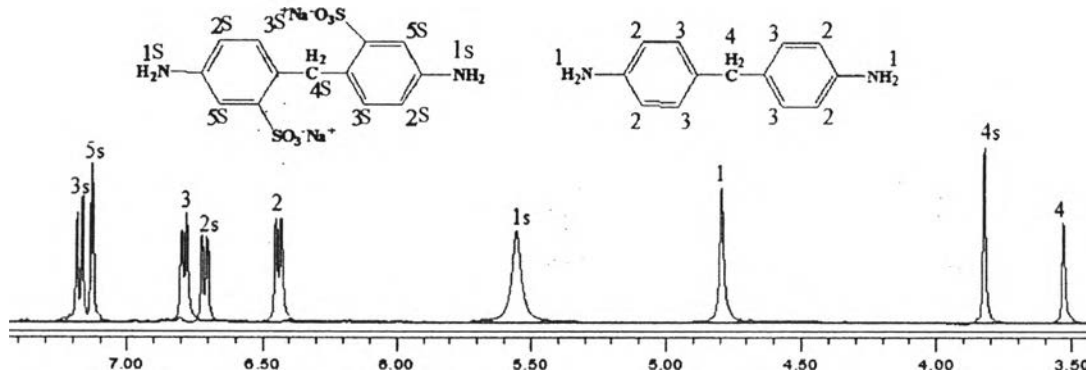


Figure G3 The ^1H -NMR spectrum of DDM and S-DDM.

Appendix H X-Ray Diffraction (XRD)

The wide angle X-ray diffraction microscope (Bruker AXS, model D8 Advance) was used to study the crystallinity of Non S-coPI and S-coPI, the S-coPI-3 was selected for a sample of sulfonated polymer membrane. The Cu K-alpha radiation source was operated at 40 kV / 30mA. K-beta filter was used to eliminate the interference peak. A divergence slit and a scattering slit of 0.5 deg together with a 0.3 mm receiving slit are set on the instrument. The film was placed into a sample holder and the measurement was continuously run. The experiment were recorded by monitoring the diffraction appearing in the 2θ range

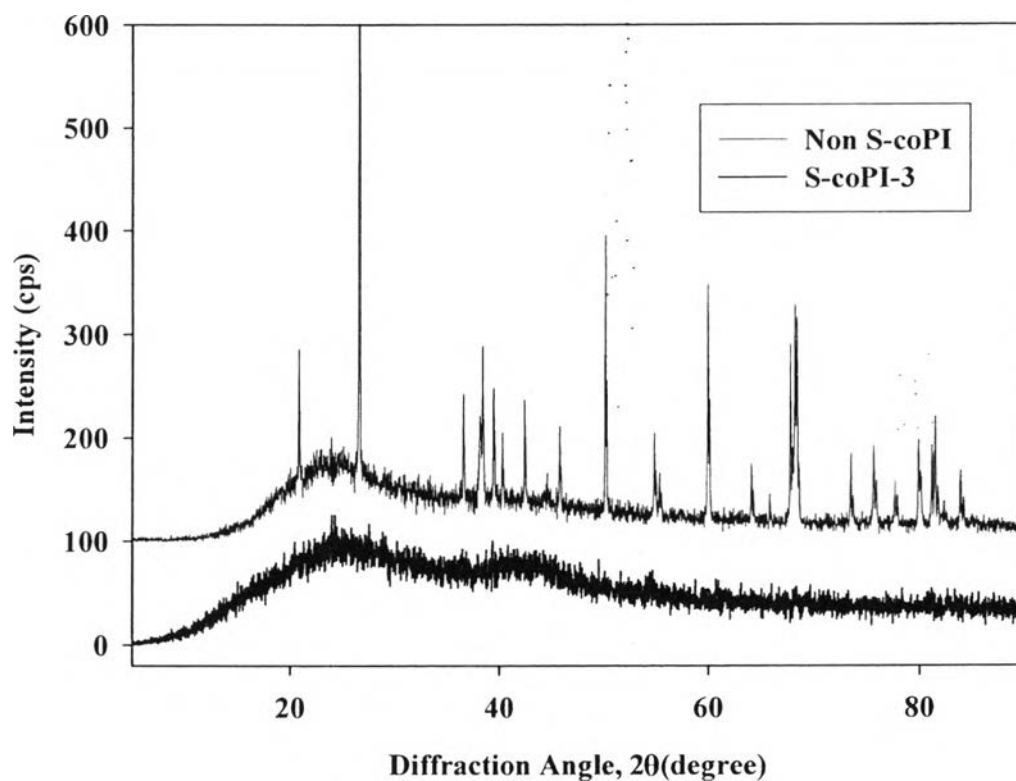


Figure H1 The XRD diffraction patterns of Non S-coPI and S-coPI-3 films.

Appendix I Degree of sulfonation (DS) and Ion Exchange Capacity (IEC)

Polymer membranes were acidified with an excess 0.1 M HCl solution at a room temperature for 24 h. Then, they were washed and dried at 80 °C for 24 h. The membranes were immersed in 50 ml of 1 M NaCl for 24h. The solution was titrated by 0.01 M NaOH using phenolphthalein as an indicator. The titrations were repeated two times, the DS and IEC value were calculated by equations I1 and I2, respectively.

$$DS(\%) = \frac{(V_{NaOH} \times M_{NaOH})/1000}{Mole\ of\ polymer\ membrane} \times 100 \quad (I1)$$

$$IEC\ (meq./g) = \frac{V_{NaOH} \times M_{NaOH}}{W_d} \quad (I2)$$

where V_{NaOH} = the volume of sodium hydroxide solution

M_{NaOH} = the concentration of sodium hydroxide solution

W_d = the weight of the dry polymer membrane

Table I1 The DS and IEC of S-coPI

Sample	DS (%)	IEC
Non S-coPI	0	0
S-coPI-1	18.450 ± 1.287	0.380 ± 0.026
S-coPI-2	34.530 ± 0.042	0.689 ± 0.001
S-coPI-3	65.585 ± 0.417	1.230 ± 0.008

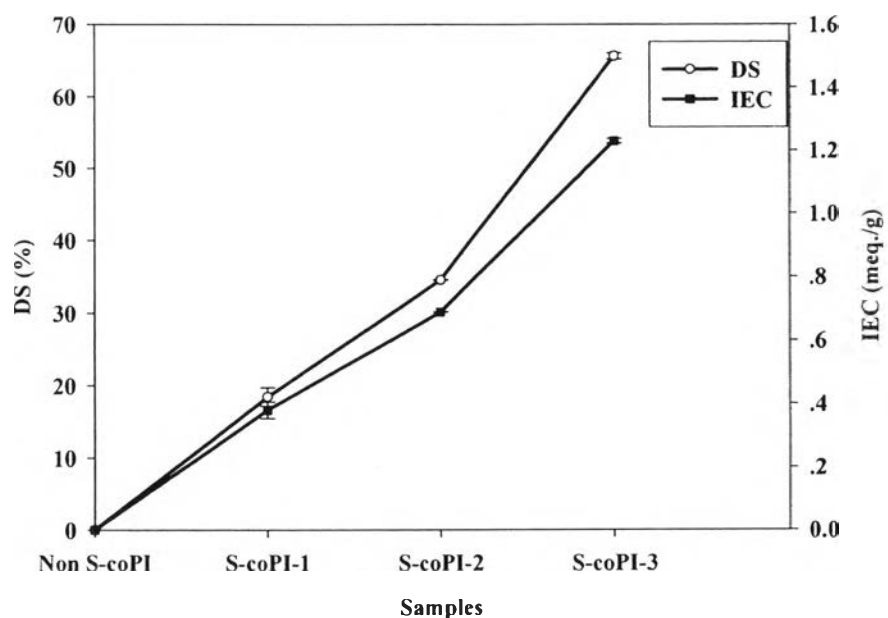


Figure 11 The DS and IEC of the S-coPI membranes.

Table I2 Raw data of the DS and IEC calculations

Sample	W _d (g)	Mole	V _{NaOH} (ml)	DS (%)	IEC
Non S-coPI	0.2541	5.411×10^{-4}	-	0	0
	0.2784	5.928×10^{-4}	-	0	0
S-coPI-1	0.2547	5.245×10^{-4}	9.2	17.54	0.361
	0.2383	4.905×10^{-4}	9.5	19.36	0.398
S-coPI-2	0.2530	5.044×10^{-4}	17.4	34.50	0.688
	0.3803	7.581×10^{-4}	26.2	34.56	0.689
S-coPI-3	0.2227	4.174×10^{-4}	27.5	65.88	1.235
	0.2787	5.223×10^{-4}	34.1	65.29	1.224

Appendix J Comparison of Polyimide Membrane Properties

S-coPI-3 has the highest selectivity value obtained from the experiment; its properties are compared with those of other polyimide membranes as shown in Table J1.

Table J1 Films comparisons

Sample name	IEC (meq/g)	Water uptake (wt.%)	σ (S/cm)	P (cm ² /s)	Φ (S s/cm ³)
S-coPI-3 ^a	1.23	11.17	1.16×10^{-2}	4.02×10^{-8}	2.89×10^5
Nafion117	0.91 ^b	20.53	^b 8.00×10^{-2}	1.74×10^{-6}	4.59×10^4
SPI 63 ^c	1.75	15.89	4.10×10^{-2}	7.34×10^{-8}	5.58×10^5
SPI-80 ^d	0.95	27.0	5.50×10^{-3}	1.13×10^{-7}	4.87×10^4
NPI(1)/SPP(70) ^e	2.00	72.0	2.07×10^{-1}	6.20×10^{-7}	3.20×10^5
PVA/10%MMT ^f	-	-	3.68×10^{-2}	3.67×10^{-6}	1.00×10^4

^athis experiment; ^bAkbarian-Feizi *et al.*, 2010; ^cWoo *et al.*, 2003; ^dPan *et al.*, 2010;
^eLi *et al.*, 2008; ^fYang *et al.*, 2009

S-coPI-3 is of the lowest methanol permeability compared with other polyimide membranes, as shown in Table J1. But it has a lower proton conductivity value than some polyimide membranes. The selectivity of S-coPI-3 is higher than Nafion117, SPI-80^d, and PVA/10%MMT^f, so the S-coPI-3 is of a higher performance than others with respect to the DMFC membrane. However, S-coPI-3 is of a lower selectivity value than SPI 63^c and NPI(1)/SPP(70)^e due to the lower proton conductivity.

CURRICULUM VITAE

Name: Mr. Naphat Taweeckarn

Date of Birth: September 28, 1986

Nationality: Thai

University Education:

2005-2008 Bachelor Degree of Science (Chemistry), Faculty of Science and Technology, Thammasat University, Pathumthani, Thailand

Proceedings:

1. Taweeckarn, N.; and Sirivat, A. (2011, April 26). Synthesis and characterization of sulfonated poly(aromatic imide-*co*-aliphatic imide) (S-coPI) membrane for direct methanol fuel cell. Proceedings of the 2nd National Research Symposium on Petroleum, Petrochemicals, and Advanced Materials and The 17th PPC Symposium on Petroleum, Petrochemicals, and Polymers, Bangkok, Thailand.

Presentation:

1. Taweeckarn, N.; and Sirivat, A. (2011, April 26). Synthesis and characterization of sulfonated poly(aromatic imide-*co*-aliphatic imide) (S-coPI) membrane for direct methanol fuel cell. Paper presented at the 2nd National Research Symposium on Petroleum, Petrochemicals, and Advanced Materials and The 17th PPC Symposium on Petroleum, Petrochemicals, and Polymers, Bangkok, Thailand.